Phytopathologia Mediterranea
The international journal of the
Mediterranean Phytopathological Union

Firenze University Press
www.fupress.com/pm

Research Papers

Biological and molecular characterization of seven *Diaporthe* species associated with kiwifruit shoot blight and leaf spot in China

Yamin DU[1,2,3,4], Xianhong WANG[4], Yashuang GUO[4], Feng XIAO[4], Yuhong PENG[4], Ni HONG[1,2,3,4], Guoping WANG[1,2,3,4,*]

[1] *College of Plant Science and Technology, Huazhong Agricultural University, Wuhan 430070, Hubei, China*
[2] *Key Lab of Plant Pathology of Hubei Province, Wuhan 430070, Hubei, China*
[3] *Key Laboratory of Horticultural Crop (Fruit Trees) Biology and Germplasm Creation of the Ministry of Agriculture, Wuhan 430070, Hubei, China*
[4] *State Key Laboratory of Agricultural Microbiology, Huazhong Agricultural University, Wuhan 430070, Hubei, China*
*Corresponding author. E-mail: gpwang@mail.hzau.edu.cn

Summary. *Diaporthe* species are significant pathogens, saprobes, and endophytes, with comprehensive host association and geographic distribution. These fungi cause severe dieback, cankers, leaf spots, blights, and stem-end rot of fruits on different plant hosts. This study, explored the occurrence, diversity and pathogenicity of *Diaporthe* spp. associated with *Actinidia chinensis* and *A. deliciosa* in the main kiwifruit production areas of China. *Diaporthe* isolates (284) derived from 106 diseased leaf and branch samples were examined. Multi-locus phylogenetic analyses and morphology of 43 representative isolates revealed that seven *Diaporthe* species were obtained, including *D. alangii*, *D. compactum*, *D. eres*, *D. hongkongensis*, *D. sojae*, *D. tectonae*, and *D. unshiuensis*. Pathogenicity tests were performed on kiwifruit fruits, leaves and branches. Koch's postulates confirmed all species were pathogenic. *D. alangii* and *D. tectonae* were the most aggressive species, followed by *D. eres*, *D. sojae*, *D. hongkongensis*, *D. unshiuensis*, and *D. compactum*. Host range evaluation showed that the seven *Diaporthe* species could also infect apricot, apple, peach, pear, and plum. This is the first report of *D. alangii*, *D. compactum*, *D. sojae*, *D. tectonae*, and *D. unshiuensis* infecting kiwifruit in China, increasing understanding of the *Diaporthe* complex causing diseases of kiwifruit plants, to assist effective disease management.

Keywords. *Actinidia*, phylogeny, pathogenicity.

OPEN ACCESS

Citation: Y. Du, X. Wang, Y. Guo, F. Xiao, Y. Peng, N. Hong, G. Wang (2021) Biological and molecular characterization of seven *Diaporthe* species associated with kiwifruit shoot blight and leaf spot in China. *Phytopathologia Mediterranea* 60(2): 177-198. doi: 10.36253/phyto-12013

Accepted: February 1, 2021

Published: September 13, 2021

Data Availability Statement: All relevant data are within the paper and its Supporting Information files.

Competing Interests: The Author(s) declare(s) no conflict of interest.

Editor: Vladimiro Guarnaccia, DiSAFA - University of Torino, Italy.

INTRODUCTION

Kiwifruit is known "the king of fruits" due to its rich nutritional content, abundant dietary fibres, balanced nutritional composition of minerals, high vitamin C content, antioxidant properties and other human health-beneficial metabolites, including carotenoids and flavonoids (Huang *et al*., 2013; Pan *et*

al., 2020; Wu *et al*., 2020). The centre of origin of kiwifruit is the mountains and ranges of southwestern China (Yue *et al*., 2020). Kiwifruit has a short history of domestication, starting from the early 20th century (Huang *et al*. 2013; Li *et al*. 2017a Wu *et al*., 2020). Through decades of domestication and substantial efforts for selection from wild plants, several important horticultural species have been commercially cultivated, including *Actinidia chinensis*, *A. deliciosa*, *A. eriantha*, and *A. arguta* (Huang *et al*., 2013; Song *et al*., 2020). *Actinidia chinensis* and *A. deliciosa* are the major species cultivated in China (Huang, 2009), which had a kiwifruit cultivation area of 240,000 ha in 2018, producing 2.55 MT of fruit, accounting for nearly 55% of the global kiwifruit (FAO, 2018; Guo *et al*., 2020a).

During the past decades, with the steadily increasing duration of kiwifruit monoculture and the rapid expansion of production, diseases have become prevalent in orchards and nurseries. Branch blight and leaf spot diseases are widespread and prevalent, and these diseases cause serious economic losses in China, and affect development of the kiwifruit industry. Accurate identification of cause of these diseases is important for development of effective biosecurity and trade policies. The most common disease symptoms observed in kiwifruit plantations consist of branch blight, leaf spot, bacterial blossom blight, and fruit rot. These symptoms are related to several fungi (Hawthorne *et al*., 1982; Pennycook, 1985; Pan *et al*., 2018) and bacteria (Zhang *et al*., 2019).

Vine decline of kiwifruit in Turkey was mainly related to *Phytophthora citrophthora* (Akilli *et al*. 2011). In Greece, the pathogens which caused distinct cankers on branches of kiwifruit were *Diaporthe neotheicola* and *Botryosphaeria dothidea* (Thomidis *et al*., 2010, 2013). *Diaporthe ambigua* and *D. austrafricana* were reported as causing cordon dieback in Chile (Díaz and Latorre, 2018). In China, the major pathogens causing branch blight were *B. dothidea*, *D. actinidiae*, *D. eres*, and *D. tulliensis* (Li *et al*., 2013; Bai *et al*., 2017).

Leaf spot of kiwifruit, caused by *Alternaria alternata*, *Diaporthe* spp., *Glomerella cingulata*, *Pestalotiopsis* spp. and *Phomosis* spp., has been previously reported in Korea and New Zealand (Jeong *et al*., 2008; Hawthorne and Otto, 2012). *Didymella bellidis* has been reported as the major cause of leaf spot in China (Zou *et al*., 2019).

The blossom blight of kiwifruit occurs in many countries. Several pathogens have been reported as the causal agents of this disease, including *Pseudomonas viridiflava*, *P. fluorescens*, *P. syringae*, *P. fluorescens P. syringae* pv. *syringae*, *P. syringae* pv. *actinidiae*, and *Botrytis cinerea* (Conn and Gubler, 1993; Koh *et al*., 2001; Shin *et al*., 2004; Young *et al*., 2009; Zhang *et al*., 2019)

Fruit rot of kiwifruit can be divided into field rot and postharvest fruit rot. Field rot, caused by *Sclerotinia sclerotiorum*, affects immature fruits on vines (Pennycook, 1985). More than seven fungi have been reported to be associated with postharvest fruit rots of kiwifruit (Beraha and O'Brien, 1979; Hawthorne *et al*., 1982; Pennycook, 1985), *Diaporthe* spp. and *Botryosphaeria* spp. were reported as the major causes of postharvest fruit rot. In New Zealand, *Botrytis cinerea* causes storage rot and *B. dothidea* causes ripening rot. *Botryosphaeria dothidea* also was the major cause of postharvest fruit rot in Iran (Nazerian *et al*., 2019). *Diaporthe actinidiae* has been reported to cause postharvest fruit rot in China, Iran, Korea, and New Zealand (Sommer and Beraha, 1975; Lee *et al*., 2001; Koh *et al*., 2005; Mousakhah *et al*., 2014; Li *et al*., 2017b). In addition, *D. ambigua*, *D. australafricana*, *D. novem*, and *D. rudis* have been reported to cause postharvest fruit rot of kiwifruit during cold storage in Chile. *Diaporthe ambigua* was also isolated from postharvest kiwifruit rots in Greece (Thomidis *et al*., 2013; 2019). *Diaporthe honkongensis* has been reported to cause stem-end rot in Turkey (Erper *et al*., 2017). *Diaporthe melonis* and *D. perniciosa* have been reported as the major pathogens causing postharvest fruit rots in New Zealand (Beraha and O'Brien, 1979; Hawthorne *et al*., 1982).

Before the advent of molecular biology technology, identification criteria for *Diaporthe* species were based on the morphological characteristics (e.g., colony appearance in cultures, size and shape of ascomata and conidiomata, sexual state and connections to the asexual state) and host specificity (Rehner and Uecker, 1994; Santos *et al*., 2011; Gomes *et al*., 2013; Guarnaccia and Crous, 2017; Yang *et al*., 2018b). Previous studies demonstrated that these characters were generally not sufficient for species level diagnoses, because some species of *Diaporthe* are not host-restricted and are capable of infecting several taxonomically unrelated host genera (Rehner and Uecker, 1994; Thompson *et al*., 2011; Elfar *et al*., 2013; Huang *et al*., 2013; Thompson *et al*., 2015). *Diaporthe helianthi*, as the causal agent of stem canker of sunflower, was first reported in the former Yugoslavia. Subsequent studies confirmed *Xanthium italicum*, *X. strumarium*, and *Arctium lappa* as weed hosts of *D. helianthi* (Thompson *et al*., 2015). Three other *Diaporthe* species, *D. gulyae*, *D. kochmanii*, and *D. kongii*, have been identified as the pathogens of sunflower stem canker (Thompson *et al*., 2011). In addition, character plasticity and cultural variation of *Diaporthe* hampered species clarification. Application of molecular data has progressed fungal species definition (Hibbett and Taylor, 2013; Yang *et al*., 2018a). *Diaporthe* species are being redefined, based on the combination of morphological,

cultural and phytopathogenic characteristics, mating types and DNA sequence data (Guarnaccia and Crous, 2017, 2018; Fan *et al*., 2018). Adoption of multi-locus phylogeny has provided clear resolution of classification and species (Udayanga *et al*., 2014).

China is an important kiwifruit-growing country and leader in kiwifruit cultivation. However, in recent years, the incidence and systematic identification of the *Diaporthe* species associated with branch blight of kiwifruit were only assessed in two orchards of Hubei and Anhui provinces. Only 36 strains were obtained and identified as *D. tulliensis*, *D. actinidiae* and *D. eres*, and it is unclear which species is responsible for the disease in different host varieties or species in different provinces (Bai *et al*., 2017). In addition, leaf spot of kiwifruit caused by *Diaporthe* species has been rarely reported in China, which makes effective prevention and control of the disease challenging. Therefore, larger scale surveys are needed to give increased understanding of the relative role of *Diaporthe* spp. in fungal branch blight and leaf spot found on kiwifruit in China.

The present sampled plants with shoot blight and leaf spot symptoms for pathogen isolation. Phylogenetic analyses based on the nuclear ribosomal internal transcribed spacer region (ITS), *translation elongation factor 1-alpha* (*EF1-α*) and *beta-tubulin* (*TUB*) genes, coupled with morphology of representative strains, were carried out to determine the diversity of pathogens. After pathogenicity determination, species associated with kiwifruit shoot and leaf blight were identified. This study has provided valuable information on pathogen ecology, as a basis for improving management strategies for these economically important diseases.

MATERIALS AND METHODS

Sampling and pathogen isolation

Surveys of incidence of shoot blight and leaf spot diseases were conducted in 16 orchards located in nine provinces of China, including Anhui, Chongqing, Henan, Hubei, Fujian, Shandong, Shanxi, Sichuan, and Zhejiang, from October 2017 to May 2019. A total of 106 samples with symptoms of shoot blight and/or leaf spot were collected from *Actinidia chinensis* ('Cuiyu', 'Donghong', 'Hongyang', 'Huangjin', 'Jinyan', and 'Longzanghong'), and *A. deliciosa* ('Cuixiang', 'Hayward', 'Jinkui', and 'Xuxiang'). Six pieces (4–5 mm^2) of wood or foliage were cut from each of the diseased tissues neighbouring the asymptomatic regions with a sterile scalpel. After surface sterilization in 1% NaOCl for 45 s, the tissues were treated in 75% ethanol for 45 s, rinsed three times in sterile distilled water for 1 min each, and then dried on sterilized filter paper (Fu *et al*., 2018). Each tissue piece was placed on potato dextrose agar (PDA; 20% diced potato, 2% dextrose, 1.5% agar, and distilled water) plates and incubated at 25°C in the dark for 3–5 d until fungal colony formation (Bai *et al*., 2015). Colonies with typical characteristic of *Diaporthe* spp. were sub-cultured onto fresh PDA plates. The obtained isolates were purified using hyphal tip or single spore methods. Mycelium plugs of purified isolates were transferred to PDA tubes, or stored in 25% glycerol at -80°C for subsequent use (Zhai *et al*., 2014).

DNA extraction, PCR amplification, and sequencing

Colonies were cultivated on PDA plates where the medium was covered with sterile cellophane which was incubated at 25°C in the dark for 5–7 d. Mycelia was scraped and placed into clean tubes. Total genomic DNA was extracted using a modified CTAB method (Freeman *et al*., 1996). The quality and quantity of DNA were confirmed visually by staining with Gel Red after electrophoresis in 1% agarose gel and visualization under UV light (λ = 302 nm) trans illumination (Udayanga *et al*., 2012; Gao *et al*., 2017). The internal transcribed spacer (ITS) region of the nuclear ribosomal genes was amplified using the primer sets ITS1/ITS4 (White *et al*., 1990), the primers EF1-728F/EF1-986R (Carbone and Kohn, 1999) were used to amplify part of *EF1-α*, and the primers Bt-2a/Bt-2b (Glass and Donaldson, 1995) were used to amplify part of *TUB*. For PCR, an aliquot of 50 μL reaction solution contained 5 μL of 10 × *Taq* buffer II (Mg^{2+} Plus) (TaKaRa), 1 μL of dNTP mixture (2.5 mM each), 1 μL of each primer, 0.5 μL of *Taq* (5U μL^{-1}), 2.0 μL of DNA template, and 39.5 μL of ddH_2O (Zhai *et al*., 2014). PCR parameters were initiated at 95°C for 5 min, followed by 35 cycles, each of denaturation at 95°C for 30 s, annealing at appropriate temperature for 30 s (56°C for ITS, 51°C for *EF1-α*, 61°C for *TUB*), and extension at 72°C for 30 s, and terminated with a final elongation step at 72°C for 10 min (Guo *et al*., 2020b). The PCR amplicons were purified and sequenced by Sangon Biotech Company, Ltd. The obtained sequences were analyzed on DNAMAN (v. 9.0; Lynnon Biosoft), and deposited in GenBank (Table 1).

Phylogenetic analyses

Novel sequences generated in this study were blasted against the NCBI's GenBank nucleotide database (www http://blast.ncbi.nlm.nih.gov/) to search for closely similar relatives for a taxonomic framework of the studied

Table 1. Sources and GenBank accession numbers of isolates included in this study.

Species	Isolate designation[a]	Host	Country	Genbank accession numbers		
				ITS	*EF1-α*	*TUB*
Diaporthe alangii	CFCC 52556*	*Alangium kurzii*	China	MH121491	MH121533	MH121573
	CFCC 52557	*Alangium kurzii*	China	MH121492	MH121534	MH121574
	CFCC 52558	*Alangium kurzii*	China	MH121493	MH121535	MH121575
	CQ155	*Actinidi chinese*	China	MT043825	MT109567	MT109603
	FJHJB57	*Actinidia chinese*	China	MT043831	MT109562	MT109615
	HB48	*Actinidia deliciosa*	China	MT043835	MT109578	MT109619
	LP-1	*Actinidia* sp.	China	KX457967	KX457964	/
	SC74	*Actinidia chinese*	China	MT043849	MT109592	MT109627
	SC83	*Actinidia chinese*	China	MT043850	MT109593	MT109628
D. ambigua	CBS 114015*	*Pyrus communis*	South Africa	KC343010	KC343736	KC343978
D. compactum	LC3078*	*Camellia sinensis*	China	KP267850	KP267924	/
	LC3083*	*Camellia sinensis*	China	KP267854	KP267928	/
	CQ130	*Actinidia deliciosa*	China	MT043824	MT109565	MT109601
	CQ178	*Actinidia chinese*	China	MT043827	MT109570	MT109606
	SC42	*Actinidia chinese*	China	MT043846	MT109589	MT109624
	SC67	*Actinidia chinese*	China	MT043848	MT109591	MT109626
D. eres	AR5193*	*Ulmus* sp.	Germany	KJ210529	KJ210550	KJ420799
	CBS 267.55	*Laburnum* × *watereri 'Vossii'*	Netherlands	KC343082	KC343808	KC344050
	CBS 101742	*Fraxinus* sp.	Netherlands	KC343073	KC343799	KC344041
	CFCC 52576	*Castanea mollissima*	China	MH121511	MH121553	MH121593
	CFCC 52578	*Sorbus* sp.	China	MH121513	MH121555	MH121595
	AH16	*Actinidia chinese*	China	MT043816	MT109564	MT109600
	HB24	*Actinidia chinese*	China	MT043833	MT109576	MT109617
	HB25	*Actinidia chinensis*	China	MT043834	MT109577	MT109618
	HN10	*Actinidia deliciosa*	China	MT043836	MT109579	MT109620
	WAI-1	*Actinidia* sp.	China	KX457969	KX 457965	/
	MJL13	*Actinidia chinensis*	China	MT043839	MT109582	MT109632
	MJL18	*Actinidia chinensis*	China	MT043841	MT109584	MT109634
	FJ11	*Actinidia chinensis*	China	MT043828	MT109559	MT109612
	SD16	*Actinidia chinensis*	China	MT043853	MT109595	MT109638
	SX24	*Actinidia deliciosa*	China	MT043854	MT109597	MT109630
D. ganjae	CBS 180.91*	*Cannabis sativa*	USA	KC343112	KC343838	KC344080
D. goulteri	BRIP 55657a	*Helianthus annuus*	Australia	KJ197290	KJ197252	KJ197270
D. hongkongensis	LC3484	*Camellia sinensis*	China	KP267906	KP267980	KP293486
	CBS 115448*	*Dichroa febrifuga*	China	KC343119	KC343845	KC344087
	CQ21	*Actinidia chinese*	China	MT043821	MT109571	MT109607
	CQ51	*Actinidia chinensis*	China	MT043822	MT109572	MT109608
	FJHJB53	*Actinidia chinensis*	China	MT043830	MT109561	MT109614
	MJL19	*Actinidia deliciosa*	China	MT043842	MT109585	MT109635
	MJL21	*Actinidia deliciosa*	China	MT043843	MT109586	MT109636
D. manihotia	CBS 505.76*	*Manihot utilissima*	Rwanda	KC343138	KC343864	KC344106
D. neoraonikayaporum	MFLUCC 14-1136*	*Tectona grandis*	Tailand	KU712449	KU749369	KU743988
D. raonikayaporum	CBS 133182*	*Spondias mombin*	Brazil	KC343188	KC343914	KC344156
D. sojae	FAU635*	*Glycine max*	USA	KJ590719	KJ590762	KJ610875
	FAU636	*Glycine max*	USA	KJ590718	KJ590761	KJ610874
	ZJUD68	*Citrus unshiu*	China	KJ490603	KJ490482	KJ490424
	CQ14	*Actinidia chinensis*	China	MT043819	MT109566	MT109602
	CQ16	*Actinidia chinensis*	China	MT043820	MT109568	MT109604

(Continued)

Table 1. (Continued).

Species	Isolate designation[a]	Host	Country	Genbank accession numbers		
				ITS	*EF1-α*	*TUB*
	FJHJB61	*Actinidia chinensis*	China	MT043832	MT109563	MT109616
	HN59	*Actinidia deliciosa*	China	MT043838	MT109581	MT109622
	SD8	*Actinidia chinensis*	China	MT043852	MT109596	MT109639
	SC90	*Actinidia chinensis*	China	MT043851	MT109594	MT109629
	ZJ5	*Actinidia chinensis*	China	MT043856	MT109599	MT109631
D. tectonae	MFLUCC 12-0777*	*Tectona grandis*	Thailand	KU712430	KU749359	KU743977
	MFLUCC 12-0782	*Tectona grandis*	Thailand	KU712431	KU749360	KU743978
	MFLUCC 13-0476	*Tectona grandis*	Thailand	KU712433	KU749362	KU743980
	MFLUCC 14-1139	*Tectona grandis*	Thailand	KU712438	KU749366	KU743985
	CQ58	*Actinidia chinensis*	China	MT043823	MT109573	MT109609
	CQ166	*Actinidia chinensis*	China	MT043826	MT109569	MT109605
D. tulliensis	BRIP 62248a*	*Theobroma cacao*	Australia	KR936130	KR936133	KR936132
D. unshiuensis	CFCC 52594	*Carya illinoensis*	China	MH121529	MH121571	MH121606
	CFCC 52595	*Carya illinoensis*	China	MH121530	MH121572	MH121607
	ZJUD51	*Citrus japonica*	China	KJ490586	KJ490465	KJ490407
	ZJUD52*	*Citrus unshiu*	China	KJ490587	KJ49046	KJ490408
	CQ7	*Actinidia chinensis*	China	MT043817	MT109574	MT109610
	CQ9	*Actinidia chinensis*	China	MT043818	MT109575	MT109611
	FJHJB22	*Actinidia chinensis*	China	MT043829	MT109560	MT109613
	HN51	*Actinidia deliciosa*	China	MT043837	MT109580	MT109621
	MJL15	*Actinidia deliciosa*	China	MT043840	MT109583	MT109633
	MJL35	*Actinidia deliciosa*	China	MT043844	MT109587	MT109637
	SC41	*Actinidia chinensis*	China	MT043845	MT109588	MT109623
	SC65	*Actinidia chinensis*	China	MT043847	MT109590	MT109625
Diaporthella corylina	CBS 121124*	*Corylus* sp.	China	KC343004	KC343730	KC343972

[a] ICMP: International Collection of Micro-organisms from Plants; FAU: Isolates in culture collection of Systematic Mycology and Microbiology Laboratory, USDA-ARS, Beltsville, Maryland, USA; BRIP: Queensland Plant Pathology herbarium/culture collection, Australia; CBS: Westerdijk Fungal Biodiversity Centre, Utrecht, The Netherlands; CFCC: China Forestry Culture Collection Center, China; LC: Corresponding author's personal collection (deposited in laboratory State Key Laboratory of Mycology, Institute of Microbiology, Chinese Academy of Sciences); MFLUCC: Mae Fah Luang University Culture Collection, Chiang Rai, Thailand; ZJUD: Zhejiang University.
* = ex-type culture.
/ = the Genbank accession number is absent.

isolates. Sequence alignments of different gene regions, including sequences obtained from this study and reference sequences based on recent studies of *Diaporthe* species, were initially carried out with the online server (http://mafft.cbrc.jp/alignment/server/index.html) (Katoh and Standley, 2013), and were then manually adjusted in MEGA v. 7 (Kumar *et al*., 2016).

An initial maximum likelihood (ML) phylogenetic analysis was conducted based on *EF1*-α sequences of 284 isolates obtained in this study and 31 reference strains including one outgroup taxon (*Diaporthella corylina* CBS121124) deposited in GenBank (Table 1) with a GTR+G substitution model by using IQ-tree v.1.6.8, to give an overview backbone phylogenetic tree for the genus *Diaporthe* (data not shown). A subset of 43 representative isolates was then selected based on the results of the general *EF1-α* analysis, and was processed through different phylogenetic analyses conducted individually for each locus and multiple sequences analyses using concatenated ITS, *EF1-α*, and *TUB*.

Multi-locus phylogenetic analyses were generated using Maximum likelihood (ML) and Bayesian inference (BI). The maximum-likelihood tree was inferred using the edge-linked partition model in IQ-tree (Nguyen *et al*., 2015; Minh *et al*., 2020). For the IQ-tree, the best evolutionary model for each partition was determined using ModelFinder (Minh *et al*., 2020). In the partition model, IQ-TREE can estimate the model parameters separately for every partition. After ModelFinder found the best partition, IQ-TREE immediately starts the

tree reconstruction under the best-fit partition model, Branch supports were assessed with ultrafast bootstrap approximation (UFBoot) of 1000 replicates (Hoang *et al*., 2017). Additionally, Bayesian inference (BI) was performed on the concatenated loci to construct phylogenies using MrBayes v. 3.2.2 (Ronquist *et al*., 2003) as described by Crous (2006). MrModeltest v. 2.3 (Nylander, 2004) was used to calculate the best-fit models of nucleotide substitution for each data partition with the corrected Akaike information criterion (AIC). Two analyses of four Markov Chain Monte Carlo (MCMC) chains were conducted from random trees with 8×10^6 generations. The analyses were sampled every 1000 generations, which were stopped once the average standard deviation of split frequencies was below 0.01. The first 25% of the trees were discarded as the burn-in phase, and the remaining trees were summarized to calculate the posterior probabilities (PP) of each clade being monophyletic. Phylogenetic trees were visualized in Figtree v.1.4.2 (Rambaut, 2014).

Morphological and growth rate analyses

Based on the results of the phylogenetic analyses, 17 representative isolates (including *D. alangii*: CQ155, FJHJB57; *D. compactum*: CQ178, SC67; *D. eres*: HN10, HB25, SX24, HB24, CQ3; *D. hongkongensis*: CQ51; *D. sojae*: CQ14, CQ78, CQ16; *D. tectonae*: CQ58, SC83; *D. unshiuensis*: CQ7, CQ9) were selected for morphological observations and growth rate assessments. Three-day-old mycelium plugs (5 mm diam.) were taken from the margins of actively growing cultures and transferred onto the centres of 9 cm diam. Petri dishes containing potato dextrose agar (PDA) or 2% tap water agar supplemented with sterile fennel stems. Cultures were incubated at 25°C with a 14 h/10 h fluorescent light/dark cycle (Guo *et al*., 2020b). Colony diameters were measured daily for 3 d to calculate mycelium growth rates (mm d^{-1}). For each representative isolate, these measurements were made in triplicate. Colony shape, density, and pigment production on PDA were noted after seven days. Generation of ascomata and conidiomata on PDA or fennel stems were examined periodically. Shape, colour, and size of asci were observed using light microscopy (Nikon Eclipse 90i or Olympus BX63), and 50 asci, ascospores, conidiophores, and conidia were measured.

Pathogenicity and host range

The 14 representative strains (*D. alangii*: CQ155, SC74; *D. compactum*: CQ178, SC67; *D. eres*: HN10, HB25; *D. hongkongensis*: CQ21, CQ51; *D. sojae*: CQ14, CQ16; *D. tectonae*: CQ166, CQ58 *D. unshiuensis*: CQ7, MJL15) were tested for pathogenicity on detached leaves or shoots of kiwifruit, and on branches of five other fruit tree species. One isolate of each species (*D. alangii*: CQ155; *D. compactum*: CQ178; *D. eres*: HN10; *D. hongkongensis*: CQ21; *D. sojae*: CQ14; *D. tectonae*: CQ58; *D. unshiuensis*: CQ7) was also inoculated onto fruits of kiwifruit to assess pathogenicity.

Leaves of *Actinidia chinensis* 'Cuiyu', wounded or unwounded, were inoculated with mycelium plugs of isolates in eight replicates, to assess the pathogenicity of representative isolates selected from the seven *Diaporthe* species. Fresh and healthy leaves were washed under running tap water followed by surface sterilization with 25% ethanol, drying with sterile tissue paper and then air-drying (Hawthorne and Otto, 2012; Mousakhah *et al*., 2014; Fu *et al*., 2018). For the wound inoculation method, the mycelium plugs (agar disks) were placed midway on each side of each leaf midrib after wounding three times by pinpricking with a sterilized needle (insect pin, 0.5 mm diam.). For the non-wound inoculation method, mycelium plugs were placed directly on the unwounded leaves. Inoculations with sterile agar plugs were used as negative controls. The experiment was conducted twice. The inoculated leaves were put into a plastic container covered with plastic film and incubated at 25 ± 1°C with a 12 h/12 h light/dark photoperiod. Symptoms and lesion lengths were recorded at 7 d after inoculation, and re-isolations were made from lesion margins to fulfil Koch's postulates.

Pathogenicity was also determined on excised segments of 1-year-old woody shoots of *A. chinensis* ' Cuiyu,' *A. chinensis* 'Jinyan', *A. chinensis* 'Hongyang', and *A. chinensis* 'Huangjin', in five replicates. Green shoots (5 – 10 mm diam.) were pruned from healthy kiwifruit vines and cut into 10 cm long segments, rinsed with tap water, surface disinfected with 75% ethanol, and then air-dried. Wounding and non-wounding inoculation methods were used. For the wounding treatment, a superficial wound (5 mm diam.) was made on each shoot segment by removing the cortex with a disinfected 5 mm diam. hole punch (Bai *et al*., 2015; Sessa *et al*., 2017). Agar plugs (5 mm diam.) from fungus cultures were inserted into the wounds, and the inoculated parts were sealed with Parafilm to maintain humidity (Mostert *et al*., 2001). For the non-wound inoculation method, the agar plugs were placed on the surface of unwounded shoots directly and the inoculated parts were sealed with Parafilm to maintain humidity. All inoculated shoots were kept in plastic containers covered with plastic film and maintained in the laboratory at 25°C. The experiment was conducted twice. Lesion lengths were measured at

10 d after inoculation, and pieces were excised from the xylem or phloem tissues under canker lesions neighbouring asymptomatic regions and were cultured to fulfil Koch's postulates.

Detached fruits of *A. deliciosa* 'Hayward' were inoculated with seven representative isolates in quadruplicate to determine isolate pathogenicity. The inoculations were conducted using wounded and non-wounded methods as previously described (Diaz *et al*., 2017; Li *et al*., 2017a). Healthy fruits were surface-sterilized with 75$^{c}/_{o}$ ethanol prior to inoculation, washed three times with sterile water, and were air-dried (Zhou *et al*., 2015; Erper *et al*., 2017). For the wounded treatment, each mycelium plug was placed on the fruit after wounding once by pinpricking with a sterilized needle (5 mm deep) (Luongo *et al*., 2011). For the non-wounded method, the mycelium plug was directly placed on the surface of unwounded fruits. Inoculation with sterile agar plugs was used as controls. Inoculation points were individually wrapped with sterilized moist cotton plugs (Zhai *et al*., 2014; Bai *et al*., 2015). Fruits were placed in a sealed plastic container at 25°C with a 12 h/12 h light/dark photoperiod. The tests were repeated twice. Seven days post inoculation, symptoms on the fruit were recorded and the lengths of lesions were measured. Recovery isolations were made from the flesh at the margins of developed lesions.

The host range of the seven *Diaporthe* species was determined on detached shoots of five *Rosaceae* fruit tree species, including *Malus pumila* 'Hong Fushi', *Prunus salicina* 'Dahongpao', *Prunus armeniaca* 'Helanxiangxing', *Pyrus pyrifolia* 'Cuiguan' and *Prunus persica* 'Youtao'. Shoots of these plants were wound-inoculated (as described above). Five shoots of each host were used for each inoculation treatment

Statistical analyses

Data from repeated tests and among treatments in each test were analyzed using SPSS Statistics 21.0 (WinWrap® Basic; http://www.winwrap.com) by one-way analysis of variance, and means were compared using Tukey's test at a significance level of $P = 0.05$.

RESULTS

Sampling and pathogen isolation

Investigations and analyses of the occurrence and sample collection of kiwifruit branch blight and leaf spot were conducted from October 2017 to May 2019. One hundred and six samples were collected from the surveyed orchards and nurseries for fungus isolations; 80 of the samples were diseased branches and 26 were infected leaves. In total, 284 *Diaporthe* isolates showed typical *Diaporthe* spp. cultural characteristics (Table 2), including fluffy, flattened, white, creamy, sulphur or grayish aerial mycelium, with solitary or aggregated, globose, dark pycnidia and the presence of alpha and/or beta conidia (Sessa *et al*., 2017; Guo *et al*., 2020b). Among them, 81 isolates were obtained from diseased leaf samples, and were identified as six species of *Diaporthe* (*D. alangii*, *D. compactum*, *D. eres*, *D. hongkongensis*, *D. sojae*, and *D. unshiuensis*). In total, 203 isolates were derived from infected shoots, and were identified as seven species of *Diaporthe* (*D. alangii*, *D. compactum*, *D. eres*, *D. hongkongensis*, *D. sojae*, *D. unshiuensis* and *D. tectonae*). The kiwifruit species and varieties from which these isolates were obtained included *A. chinensis* 'Cuiyu', 'Donghong', 'Hongyang', 'Huangjin', 'Jinyan',

Table 2. Sampling regions and numbers of *Diaporthe* isolates obtained in this study.

Sampling province	Number of isolates	Numbers of isolates from each species						
		Diaporthe unshiuensis	*D. eres*	*D. sojae*	*D. hongkongensis*	*D. compactum*	*D. alangii*	*D. tectonae*
Chongqing	92	39	19	22	7	2	1	2
Fujian	72	43	8	12	7	1	1	0
Henan	15	3	8	4	0	0	0	0
Hubei	30	4	11	8	4	1	2	0
Shanxi	17	0	17	0	0	0	0	0
Sichuan	30	2	17	7	0	2	1	1
Shandong	8	0	7	1	0	0	0	0
Zhejiang	4	1	0	3	0	0	0	0
Anhui	16	8	7	0	1	0	0	0
Total	284	100	94	57	19	6	5	3

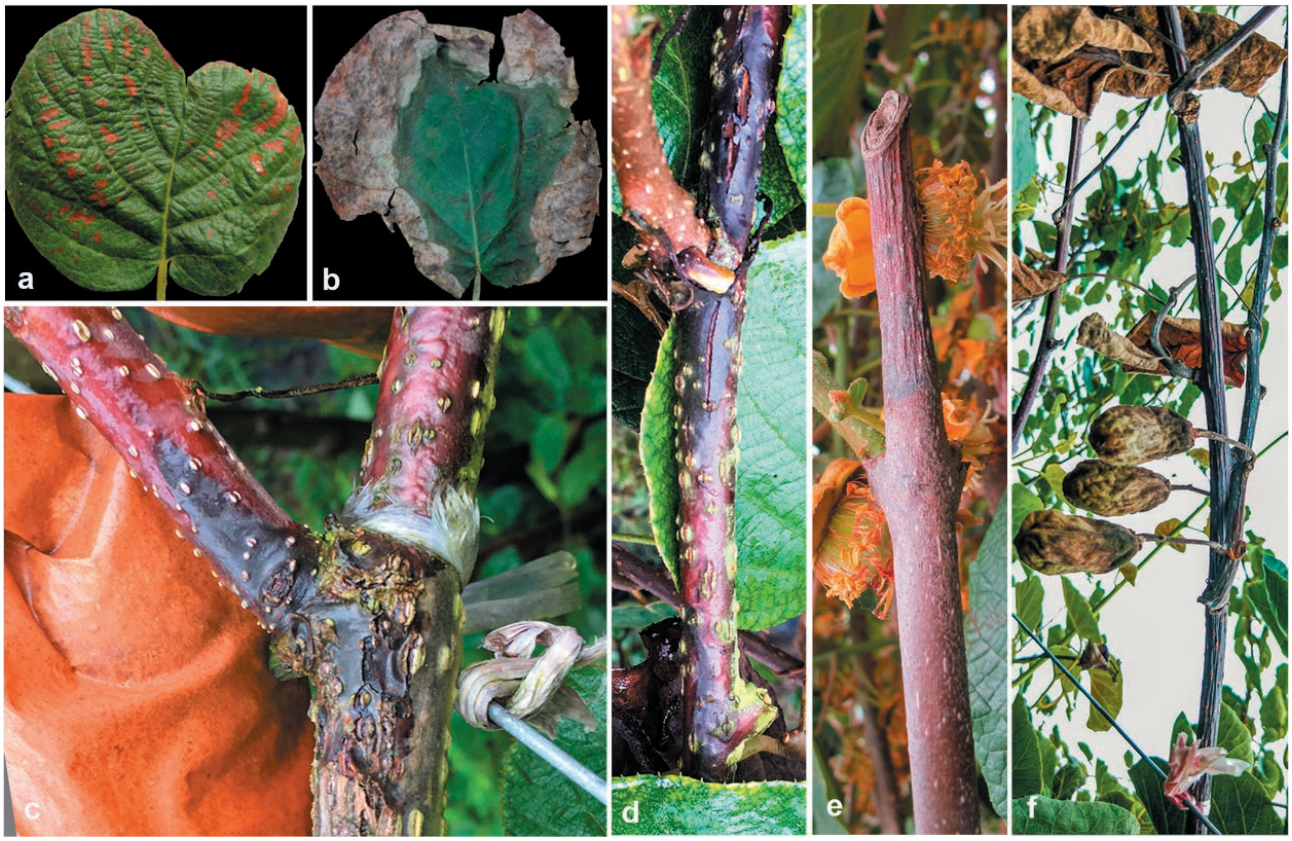

Figure 1. Typical symptoms of kiwifruit leaf spot and shoot blight. a, reddish brown spots on a leaf; b, lesions extend to the margin of a leaf, and small, black pycnidia on the necrotic parts; c, maroon and fusiform lesions on a branch; d, red-black fusiform lesions with internal discolouration formed on a branch; e, necrotic lesions spreading on a branch from the pruning wound; f, whole branch wilted.

'Longzanghong', and *A. deliciosa* 'Cuixiang', 'Hayward', 'Jinkui', and 'Xuxiang'. Branch blight symptoms were commonly observed at the incision or pruned positions, with reddish-black fusiform or irregular necrotic lesions (Figure 1c); the lesions would gradually expand along each incision (Figure 1e). Under dry climate conditions, the infected branches turned brown and cracked, with internal discolourations (Figure 1d). Whole branches were withered (Figure 1f). The diseased leaves developed silvery gray or bronze spots, which were sporadically distributed on the leaves (Figure 1a). In the later stage of disease development, the spots were expanded to the edges of the leaves, and the leaves withered and curled at their margins. Scattered pycnidia were observed on the diseased leaves (Figure 1b).

Phylogenetic analyses of isolated fungi

The 43 representative isolates were subjected to multi-locus phylogenetic analyses with concatenated ITS, *EF1-α*, and *TUB* sequences together with 31 reference isolates from previously described species, including the outgroup sequence of *Diaporthe corylina* (culture CBS 121124). A total of 1557 characters (ITS: 1–541, *EF1-α*: 542–935, *TUB*: 936–1557) were included in the phylogenetic analyses. For the Bayesian analyses, the following priors were set in MrBayes for the different data partitions: the SYM+I+G model with invgamma-distributed rates was implemented for ITS; The GTR+G model with gamma-distributed rates was implemented for *EF1*-α; and the HKY +G model with propinv-distributed rates was implemented for *TUB*. For the IQ-tree inference, the SYM+I+G model was selected for ITS, GTR+I+G for *EF1*-α, and HYK+I+G for *TUB*. Bayesian posterior probability (*PP* ≥ 0.5) and Maximum likelihood bootstrap values (ML ≥50) were shown at the dendrogram nodes (Figures 2 and 3).

The multi-locus phylogenetic results showed that 43 representative isolates were assigned to seven species (Figure 2). Five isolates grouped with the type strain and other reference sequences of *D. alangii* (Bayesian posterior probability = 0.52, Maximum likelihood bootstrap

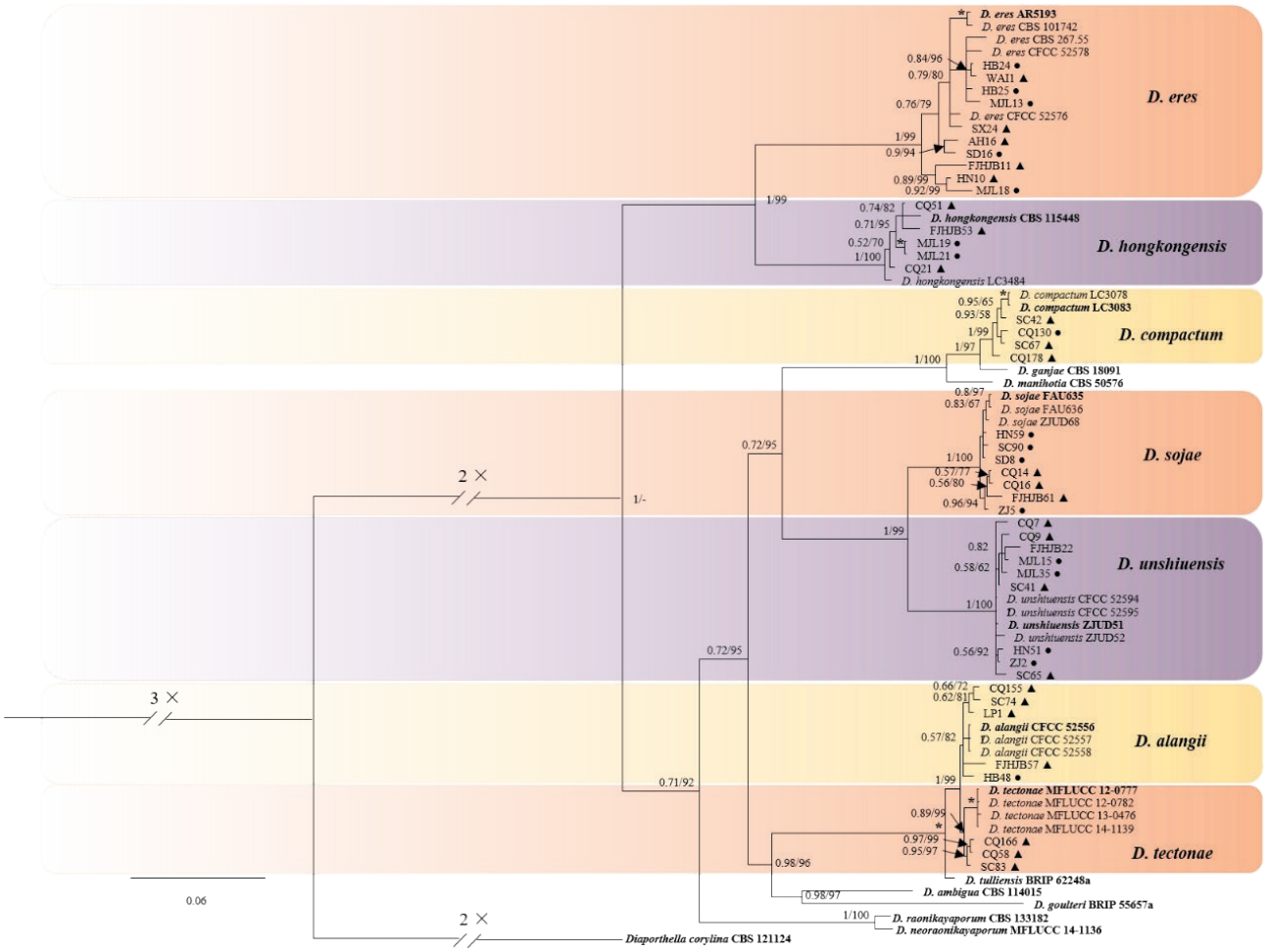

Figure 2. Maximum-likelihood phylogenetic analysis obtained from the combined ITS, *EF1-α* and *TUB2* sequence alignments of 43 *Diaporthe* isolates. The species *Diaporthella corylina* (CBS 121124) was used as the outgroup. Bayesian posterior probability (PP ≥ 0.90), and bootstrap support values > 50% are shown at the nodes. (ML ≥ 50%) were shown at the nodes (PP/ML). Asterisks (*) indicates full support (1/100). Ex-type strains were indicated in bold font. The scale bar indicates 0.06 expected changes per site. Isolate numbers accompanied by circle symbols indicate strains isolated from leaves, and triangle symbols indicate strains isolated from branches.

value 89). Four isolates clustered together with the type strain and other reference strains of *D. compactum* with high support (1.00, 99). Ten isolates clustered together with the ex-type strain and other reference strains of *D. eres* with high support (1.00, 99). Five isolates grouped with the ex-type strain and other reference strains of *D. hongkongensis* with strong support (1.00, 100). Seven isolates clustered together with the type strain and other reference strains of *D. sojae* with strong support (1.00, 100). Three isolates grouped with the reference strains of *D. tectonae* with high support (0.89, 99). Nine isolates were identified as *D. unshiuensis*, forming a highly supported subclade (1.00, 100).

The individual alignments and trees of the three single loci used in the analyses were also compared with respect to their performance in species recognition. Each gene used differentiated *D. compactum, D. eres, D. hongkongensis, D. sojae, and D. unshiuensis*. Moreover, ITS and *EF1-α* gathered *D. tectonae* and *D. alangii* into one clade (data not shown). The phylogenetic analysis of *TUB* sequences showed that similar clades statuses compared with the phylogenetic analyses based on the concatenated ITS, *EF1-α*, and *TUB* sequences (Figure 3). The phylogenetic analysis of *TUB* sequences was conducted with a HKY+I+F substitution model using IQ-tree v.1.6.8, and 436 characters were included in the phylogenetic analysis.

Morphological and growth rate analyses of isolates

Morphological observations coupled with phylogenetic analyses were used to clarify the species delimi-

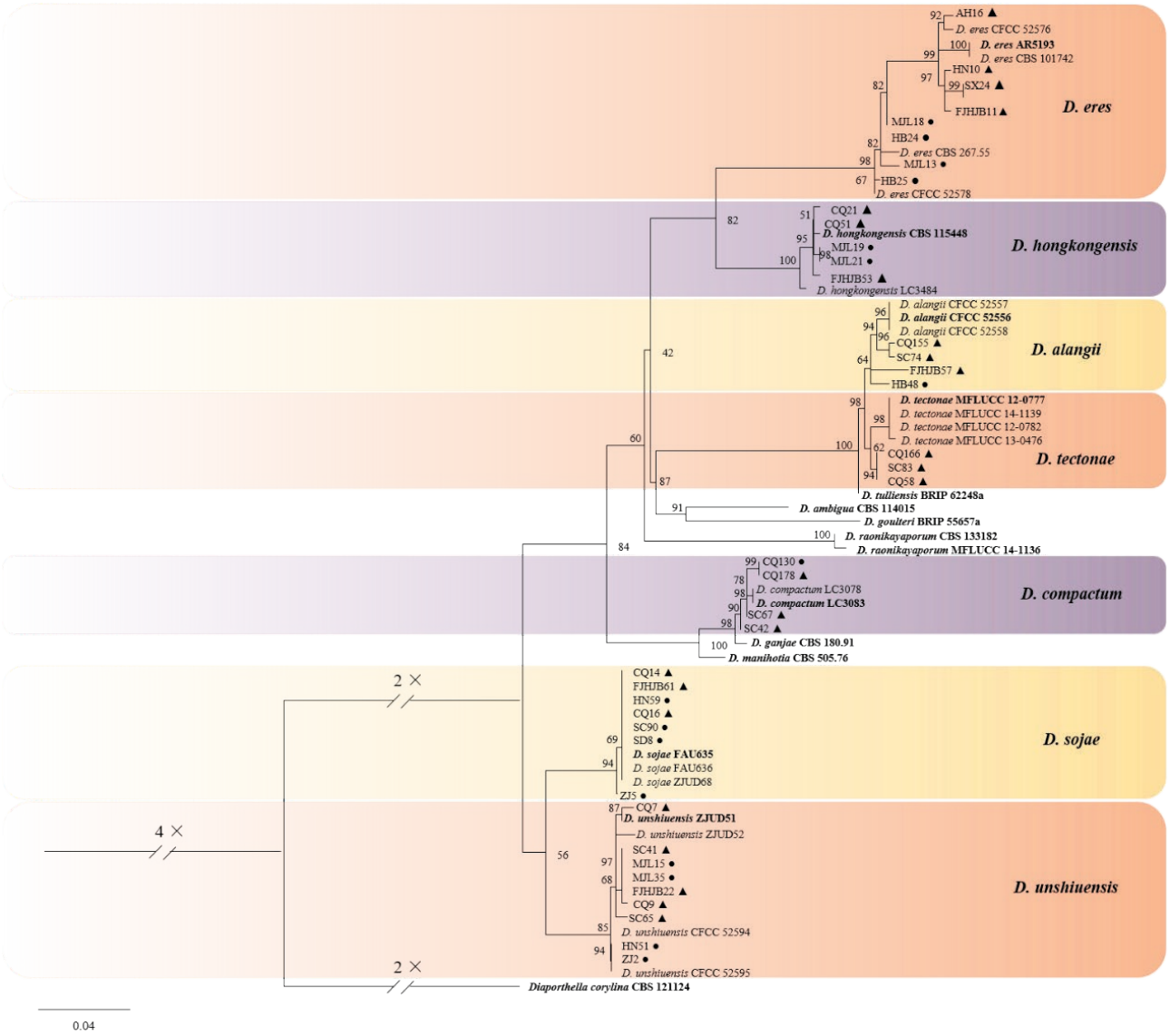

Figure 3. Maximum likelihood tree based on *TUB* sequences from 43 *Diaporthe* isolates. The species *Diaporthella corylina* (CBS 121124) was used as the outgroup. Bootstrap support values > 50% are shown at the nodes. Ex-type strains are indicated in bold font. The scale bar indicates 0.04 expected changes per site. Circle symbols indicate strains isolated from leaves, triangle symbols indicate strains isolated from branches.

tations. The morphological characteristics of the representative isolates of *Diaporthe* spp. recovered in this study were as follows:

Diaporthe sojae. Colonies on PDA had flattened mycelium and brown accumulation of pigment (Figure 4a), and colony diam. was 23–38 mm after 3 d at 25°C. Black or brown conidiomata were separated or aggregated on the colony surfaces of PDA (Figure 4b). Translucent spiral conidial cirri extruded from ostioles (Figure 4j). In the asexual state, two types of conidia were observed. Alpha conidia were hyaline, cylindrical, aseptate, biguttulate, rounded at each end (Figure 4s), 6–8 × 3–4 µm, mean ± SD = 7.0 ± 0.5 × 3.4 ± 0.3 µm. Beta conidia were filiform, hyaline, straight or hamate, aseptate, each with the base slightly inflated, tapering towards one apex (Figure 4s), 14–30 × 2–3 µm, mean ± SD = 23.9 ± 3.2 × 2.4 ± 0.2 µm. Conidiophores were phialidic, hyaline, terminal, cylindrical, 16–21 × 1.5–4 µm, tapered towards the apices (Figure 4II), Tapering perithecial necks protruded through substrata deeply immersed in fennel stem tissues (Figure 4i). Asci were unitunicate, eight-spored, sessile, elongate to clavate

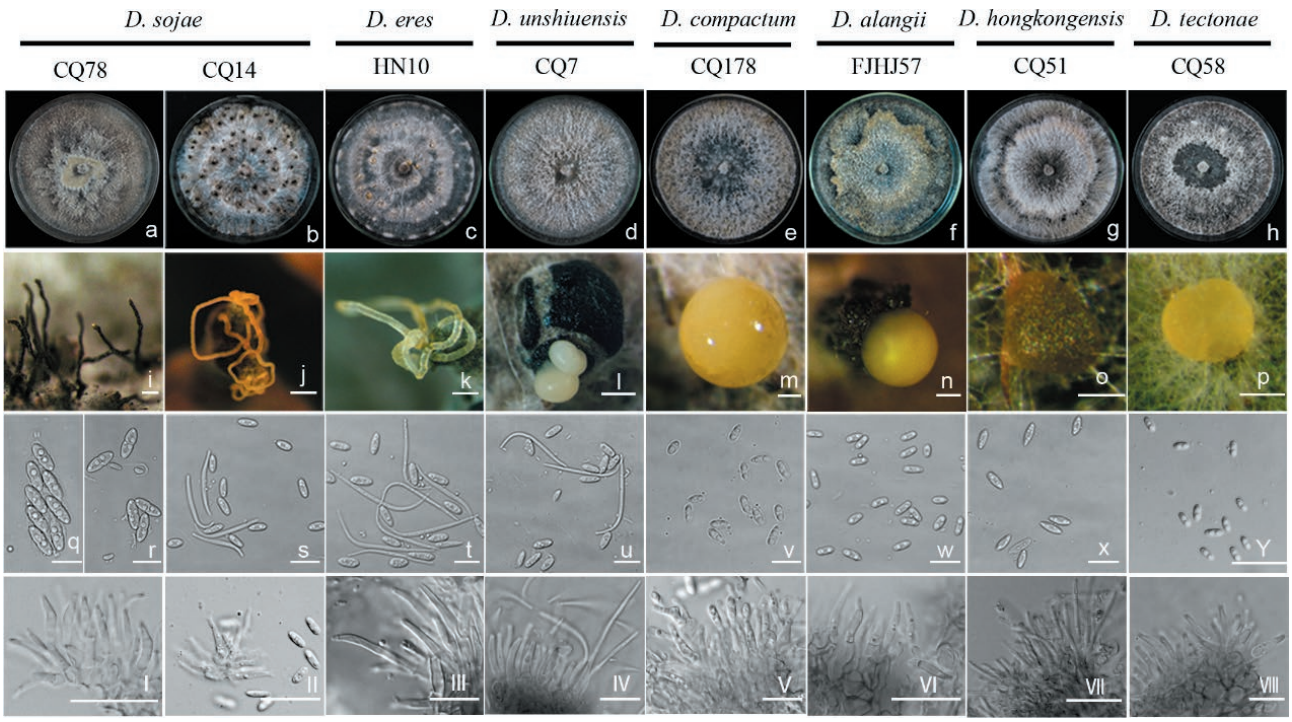

Figure 4. Morphologies of representative isolates selected from seven *Diaporthe* species. a to h, colony characteristics of the representative isolates of belonging to seven species cultured on potato dextrose agar incubated at 25°C in darkness. i, ascomata on fennel stems. j and k, spiral conidial cirri. l to p. conidial droplets. q, asci. r, ascospores. s to u, alpha and beta conidia. v to y, alpha conidia. I-VIII, conidiophores. Scale bars: i, k and n = 200 μm; j and l = 500 μm; m, o and p =100 μm; q to y = 10 μm. I to III and VI to VII = 20 μm; IV, V, and VIII =10 μm.

(Figure 4q), ascospores were hyaline, two-celled, often four-guttulate. *Conidiophores* phialidic, hyaline, terminal, ampulliform, 15–23 × 1.5–3.5 μm, tapered towards the apex (Figure 4I). Compared with the description of the ex-type isolate FAU 635, the asci of isolate CQ78 were slightly shorter (32.5–45.5 × 8–12 vs 38.5–46.5 × 7–9 μm; mean ± SD = 38.2 ± 2.9 × 10.0 ± 0.8 μm), and the ascospore were of similar size to the ex-type isolate (10–13 × 4–5 vs 9.5–12 × 3–4 μm), mean ± SD = 11.0 ± 0.7 × 4.3 ± 0.3 μm (Table 3). Of all species obtained from this study, only *D. sojae* produced the sexual state on fennel stems *in vitro*.

Diaporthe eres. Cultures appeared initially as white (surface) and pale yellowish to brownish at the centres with age, colony diam. 25–31 mm in 3 d at 25°C. Aerial mycelia were white, sparse and fluffy. Each colony on PDA contained no less than two wide concentric rings of conidiomata at maturity (Figure 4c). Conidiomata were subglobose to globose, dark brown to black, with spiral conidial cirri extruding from ostioles (Figure 4k). Alpha conidia were hyaline, fusiform or oval (Figure 4t), 7–11 × 3–5 μm, mean ± SD = 8.6 ± 0.9 × 3.7 ± 0.4 μm. Beta conidia were hyaline, filiform, smooth, curved, with truncate bases (Figure 4t), 30–43 × 2–3 μm, mean ± SD = 34.88 ± 3.56 × 2.35 ± 0.34 μm. Conidiophores were phialidic, hyaline, terminal, cylindrical, 9–13 × 1.5–4 μm, tapered towards the apices (Figure 4III).

Diaporthe unshiuensis. Aerial mycelia were white, sparse, turning to grey with age, and with light gray pigmentation at the colony centres (Figure 4d), with colony diam. 23–28 mm in 3 d at 25°C. Conidiomata were subglobose, black and solitary or aggregated on the medium surface, with opalescent, glossy conidial drops exuding from the ostioles (Figure 4l). Alpha conidia were hyaline, ellipsoidal or clavate, smooth, and aseptate (Figure 4u), 6–8 × 2–4 μm, mean ± SD = 7.0 ± 0.5 × 3.0 ± 0.3 μm. Beta conidia were filiform, hyaline, smooth, curved, with truncate bases (Figure 4u), 22–40 × 2–3 μm, mean ± SD = 28.8 ± 3.5 × 2.2 ± 0.3 μm. Conidiophores were phialidic, hyaline, terminal, and cylindrical, 15–26 × 1.5–2.5 μm, and tapered towards the apices (Figure 4IV).

Diaporthe compactum. Cultures were entirely white from above, and brown, and feathery from below, with neat margins (Figure 4e), and colony diam. 27–30 mm after 3 d at 25°C. Brown or pale gray and spheroidal conidiomata were semi- or fully-embedded in the media, and conidia exuded from ostioles in lustrous, yellowish drops (Figure 4m). Alpha conidia were fusiform, hya-

Table 3. Sizes of alpha and beta conidia, and growth rates in culture, of representative isolates of *Diaporthe* spp. obtained in this study.

Species, isolate	Conidium sizes						Growth rate (mm d^{-1})
	Alpha conidia [a]		Beta conidia[b]		Means ± SD of conidia[c]		
	Length (µm)	Width (µm)	Length (µm)	Width (µm)	α-Conidia	β-Conidia	
Diaporthe eres							
HN10	6.56–11.23	3.18–4.88	29.43–43.23	1.69–3.11	8.59 ± 0.86 × 3.69 ± 0.35	34.88 ± 3.56 × 2.35 ± 0.34	10.1
HB25	6.85–10.27	3.18–4.13	26.26–41.96	1.74–3.83	7.91 ± 0.64 × 3.70 ± 0.24	34.42 ± 0.45 × 2.53 ± 0.37	9.2
SX24	6.06–8.52	2.81–4.13	20.91–32.30	1.44–3.09	7.30 ± 0.52 × 3.60 ± 0.28	27.53 ± 2.70 × 2.14 ± 0.30	8.3
HB24	5.86–8.48	2.76–4.70	/	/	7.24 ± 0.58 × 3.67 ± 0.38	/	8.5
CQ3	5.22–7.61	2.75–3.53	/	/	6.44 ± 0.60 × 3.11 ± 0.19	/	11.7
D. hongkongensis							
CQ51	6.97–10.39	3.07–4.65	/	/	8.47 ± 0.76 × 3.78 ± 0.33	/	9.8
D. sojae							
CQ14	5.57–8.27	2.82–4.05	14.43–30.54	1.67–3.29	6.98 ± 0.52 × 3.42 ± 0.29	23.89 ± 3.19 × 2.38 ± 0.16	7.6
CQ78	6.19–9.17	3.10–5.00	/	/	7.81 ± 0.76 × 3.92 ± 0.42	/	12.5
CQ16	6.16–8.11	2.11–3.56	/	/	7.15 ± 0.48 × 2.95 ± 0.27	/	9.8
D. unshiuensis							
CQ7	5.82–8.74	2.40–3.50	21.98–41.15	1.47–2.71	6.96 ± 0.52 × 3.00 ± 0.27	28.77 ± 3.48 × 2.15 ± 0.32	9.3
CQ9	5.81–8.81	2.59–4.05	18.31–30.97	1.85–3.19	7.27 ± 0.67 × 3.28 ± 0.30	25.48 ± 2.18 × 2.88 ± 0.28	7.8
D. tectonae							
CQ58	4.38–7.09	2.11–3.28	/	/	5.60 ± 0.58 × 2.64 ± 0.30	/	12.3
SC83	5.65–6.86	2.56–3.42	/	/	7.91 ± 0.64 × 3.70 ± 0.24		10.4
D. compactum							
CQ178	6.19–8.52	2.98–4.24	/	/	7.27 ± 0.52 × 3.73 ± 0.28	/	9.6
SC67	6.19–10.01	2.75–4.40	/	/	7.86 ± 0.54 × 3.53 ± 0.31	/	8.6
D. alangii							
CQ155	5.44–9.28	2.33–4.13	22.33–40.86	1.42–4.00	7.55 ± 0.85 × 3.21 ± 0.45	32.67 ± 4.99 × 2.49 ± 0.49	9.8
FJHJB57	5.72–10.14	2.77–4.45	/	/	7.20 ± 0.76 × 3.64 ± 0.35	/	8.1

[a] Minimum and maximum lengths and widths of 50 alpha conidia.
[b] Minimum and maximum lengths and widths of 50 beta conidia.
[c]: Mean conidium sizes of calculated from statistical analyses. Data were analyzed with SPSS Statistics 21.0 (WinWrap Basic; http://www.winwrap.com) by one-way analysis of variance, and means were compared using Duncan's test (at $P = 0.05$). SD = standard deviation.
/ indicates where beta conidia were not produced.

line, usually biguttulate, straight or slightly curved, and both ends of each conidium were blunt, or one end was rounded and the other acute (Figure 4v), 6–9 × 3–4 µm, mean ± SD = 7.3 ± 0.5 × 3.7 ± 0.3 µm. Beta conidia were not observed. Conidiophores were phialidic, hyaline, terminal, ampulliform, and tapered towards their apices, 9–17 × 1–3 µm (Figure 4V).

Diaporthe alangii. Aerial mycelium was sparse. Colonies were white at first, and becoming light brown due to pigment formation, with neat or petaloid margins (Figure 4f), colony diam. 24–30 mm after 3 d at 25°C. Conidiomata were scattered, black or brown and irregularly distributed over agar surfaces, with yellowish conidial drops exuding from the ostioles (Figure 4n). Alpha conidia were aseptate, hyaline, biguttulate, each usually with one end obtuse and the other acute (Figure 4w), 6–10 × 3–5 µm, mean ± SD = 7.2 ± 0.8 × 3.6 ± 0.4 µm. Beta conidia were not observed. Conidiophores were phialidic, hyaline, terminal, ampulliform, tapered towards the apices, 9–18 × 1.5–2.5 µm (Figure 4VI).

Diaporthe hongkongensis. Colonies were snow-white, with dense aerial mycelium, which collapsed in the center, and the collapsed parts were moist and sticky (Figure 4g), colony diam. 30 mm after 3 d at 25°C. Conidiomata were spheroidal and enveloped by tangled mycelia. Irregular and yellowish conidial piles were effusing from the ostioles (Figure 4o). Alpha conidia were fusiform, hyaline, septate, and not obtuse at both ends (Figure 4x), 7–10 × 3–5 µm, mean ± SD = 8.5 ± 0.8 × 3.8 ± 0.3 µm. Beta conidia was not observed. Conidiophores were phialidic, hyaline, terminal, cylindrical, tapered towards their apices, 25–30 × 1–3 µm (Figure 4VII).

Diaporthe tectonae. Colonies were white at first, with gray pigmentation gradually accumulating in the centres until entire colony colonies turned brown (Figure 4h), colony diam. 31–36 mm after 3 d at 25°C. Conidiomata globose, black or brown, scattered, erumpent on PDA, with conidial droplets exuding from the centre ostioles (Figure 4p). Alpha conidia were cylindrical or fusiform, hyaline, usually biguttulate, and septate (Figure 4y), 4–7 × 2–3 µm, mean ± SD = 5.6 ± 0.6 × 2.6 ± 0.3 µm. Beta conidia were not observed. Conidiophores phialidic, hyaline, terminal, ampulliform, and tapered towards their apices, measuring 11–20 × 1.5–3 µm (Figure 4VIII).

Pathogenicity tests

Two typical symptoms developed on detached leaves of *A. chinensis*, which were observed at the wound sites at 7 d post inoculation. One symptom consisted of reddish-brown, round or suborbicular, small, slowly expansion lesions, while the other consisted of lesions with black necrotic centres surrounded by round or suborbicular brown halos (Figure 5a). The first of these symptoms developed after inoculations with *D. compactum*, *D. eres*, *D. sojae* or *D. unshiuensis*, while the second was induced by inoculations with *D. tectonae*, *D. alangii* or *D. hongkongensis*. Lesion diameters caused by the different fungi differed significantly. *Diaporthe tectonae*, or *D. alangii* caused large lesions (mean diam. = 10–22 mm) on all the inoculated leaves, those caused by *D. hongkongensis* or *D. eres* were smaller (5–8 mm), while those caused by isolates of *D. sojae*, *D. compactum*, or *D. unshiuensis* were smaller still (2–4 mm) (Figure 6a). Unwounded leaves inoculated with *Diaporthe* spp. isolates remained symptomless. In parallel, no lesions were observed on the leaves that were wound and non-wound inoculated with PDA discs as controls. Koch's postulates were fulfilled by re-isolating each *Diaporthe* sp. isolate only from symptomatic leaves.

In the pathogenicity tests conducted on branches of four kiwifruit varieties, all the *Diaporthe* species were pathogenic to wounded branches. The symptoms induced by representative isolates were similar, as fusiform necrotic lesions and internal discolouration observed at the wound sites (Figure 5b). The lesion lengths caused by the representative isolates tested on different cultivars were diverse. *Diaporthe tectonae* and one isolate of *D. alangii* (SC74) induced large lesions (mean length = 67–83 mm) on *A. chinensis* 'Huangjin', *D. alangii* (CQ155) or *D. eres* caused smaller lesions (20–30 mm), and the other pathogens induced even smaller (2–18 mm) (Figure 6b). *Diaporthe tectonae*, *D. alangii*, and a *D. sojae* isolate (CQ16) caused large lesions (50–106 mm) on *A. chinensis* 'Hongyang', while the remaining isolates caused shorter lesions (4–20 mm) (Figure 6c). *Diaporthe tectonae* or *D. alangii* (SC74) induced large lesions (39–54 mm) on *A. chinensis* 'Jinyan', while *D. eres* (HB25) and *D. alangii* (CQ155) caused smaller lesions on this cultivar (17–22 mm). The remaining isolates caused short lesions on this cultivar (5–12 mm) (Figure 6d). *Diaporthe tectonae* and a *D. alangii* isolate (SC74) caused large lesions (40–68 mm) on *A. chinensis* 'Cuiyu', *D. alangii* (CQ155), *D. compactum* (CQ178), *D. eres* (HB25), or *D. sojae* (CQ16) caused shorter lesions (15–25 mm), and those from the remaining isolates were shorter still (3–10 mm) (Figure 6e). Unwounded shoots of kiwifruit inoculated with *Diaporthe* spp. isolates remained symptomless, and no lesions developed on the shoots that were wound and non-wound inoculated with PDA discs. Each respective *Diaporthe* species was re-isolated from inoculated symptomatic shoots, fulfilling Koch's postulates for these pathogens.

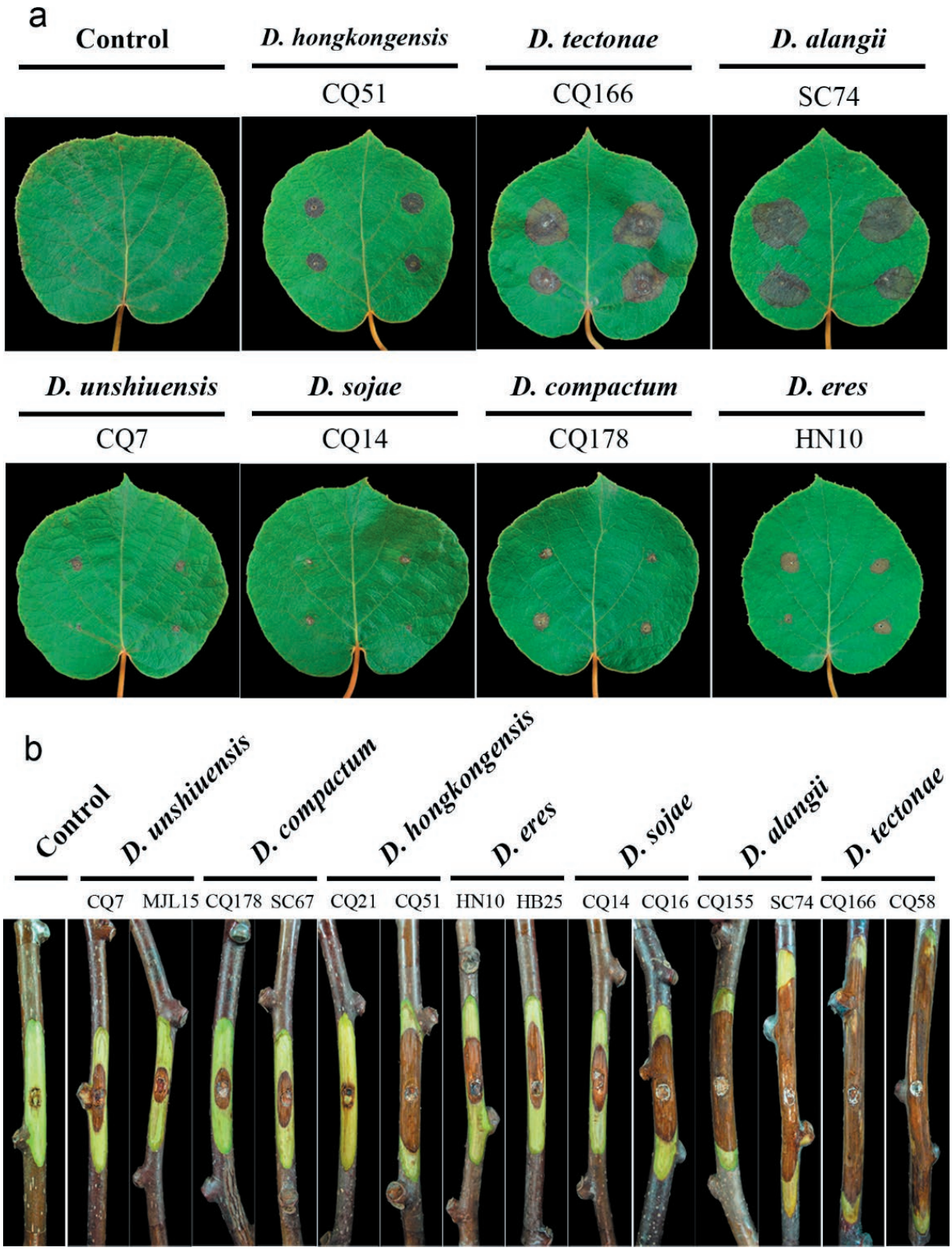

Figure 5. Pathogenesis of seven *Diaporthe* species on kiwifruit leaves and stems. a, symptoms caused after inoculation of wounded kiwi leaves (*Actinidia chinensis* 'Cuiyu') with mycelium plugs from cultures of seven *Diaporthe* spp. b, symptoms caused by inoculation of wounded kiwi branches (*Actinidia chinensis* 'Hongyang') with mycelium plugs from cultures of seven *Diaporthe* spp.

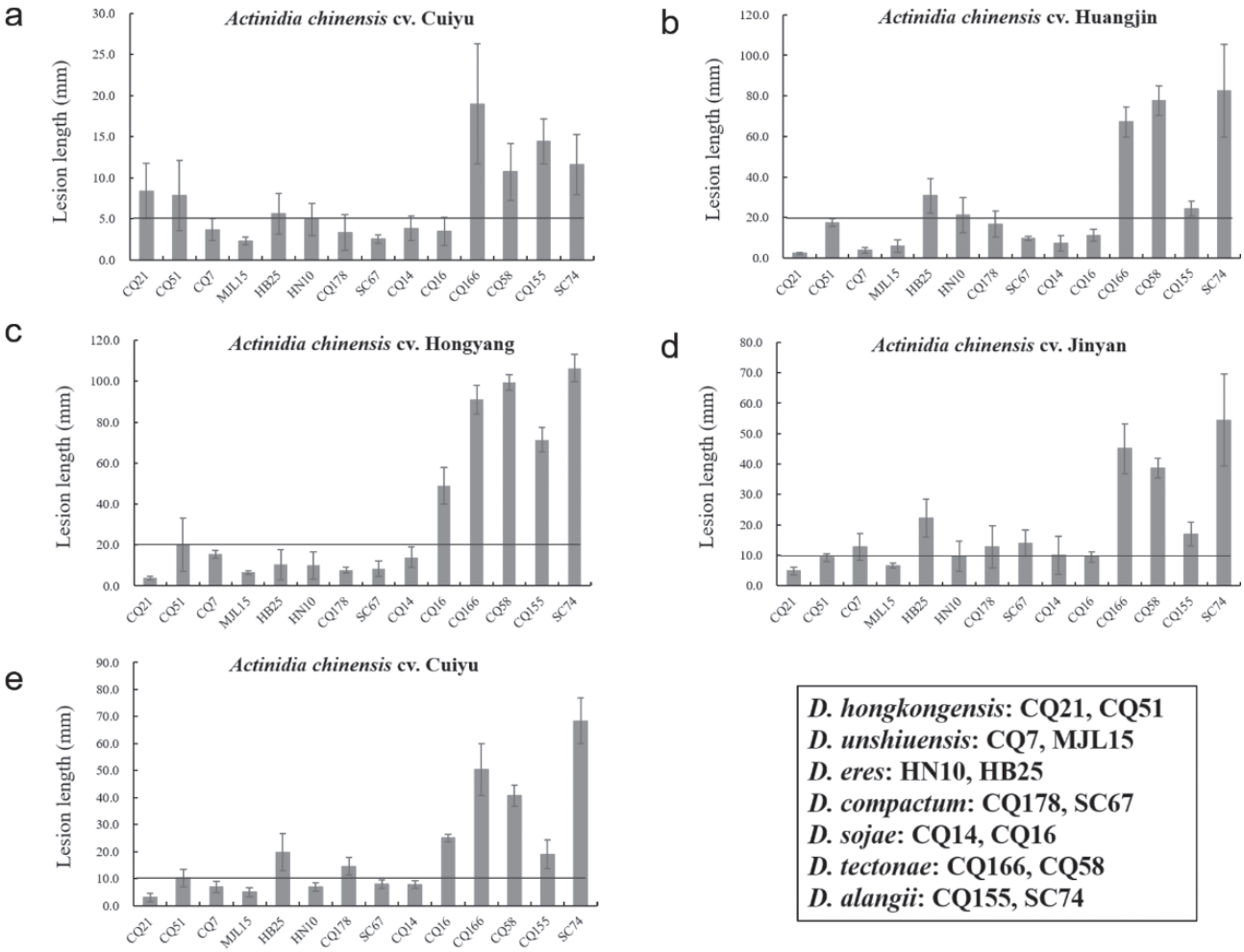

Figure 6. Mean lesion lengths on wounded kiwifruit leaves and shoots at 10 dpi with mycelium plugs of representative isolates of seven *Diaporthe* species. a, lesion length on wounded leaves of *Actinidia chinensis* 'Cuiyu'. b to e, lesion lengths on the wounded kiwifruit shoots (*Actinidia chinensis* 'Huangjin', *Actinidia chinensis* 'Hongyang', *Actinidia chinensis* 'Jinyan', or *Actinidia chinensis* 'Cuiyu'.

Fruits were susceptible to the representative isolates selected from each species, and all tested species caused rots on wounded fruits. Typical symptoms were some sarcocarp tissues swollen with internal softening around the inoculation wounds at early stages, transparent drops streaming from the inoculation punctures, epidermis peeling, and brownish, damp and rotted flesh (Figure 7a). Fruits inoculated with *D. alangii* (CQ155), *D. eres* (HN10), *D. sojae* (CQ14), *D. tectonae* (CQ58), or *D. hongkongensis* (CQ21) had larger lesions (mean diam. = 30–42 mm) than those inoculated with *D. unshiuensis* (CQ7) or *D. compactum* (CQ178), (13–17 mm) (Figure 7b). All the non-wounded fruits inoculated with *Diaporthe* spp. isolates remained symptomless. The negative controls of wounded and unwounded fruits did not produce lesions. Each respective *Diaporthe* species was re-isolated from the symptomatic fruits, fulfilling Koch's postulates for these pathogens.

In the host range tests, at 10 d post-inoculation, the seven *Diaporthe* species all caused canker symptoms on detached shoots of the five different fruit crop plants. After removing phloem tissues, maroon and fusiform necrotic lesions emerged in the underlying wood below, and these extended along the inoculated branches. In most cases, the affected shoots of pear and apple showed swollen and the bark cracking at the margins, with dark-brown to reddish cankers and abundant gummosis were observed at the inoculation sites on the branch of plum and apricot. The symptoms produced on peach shoots were black depressed cankers. The *Diaporthe* isolates caused different degrees of lesioning on detached branches of the different fruit tree species.

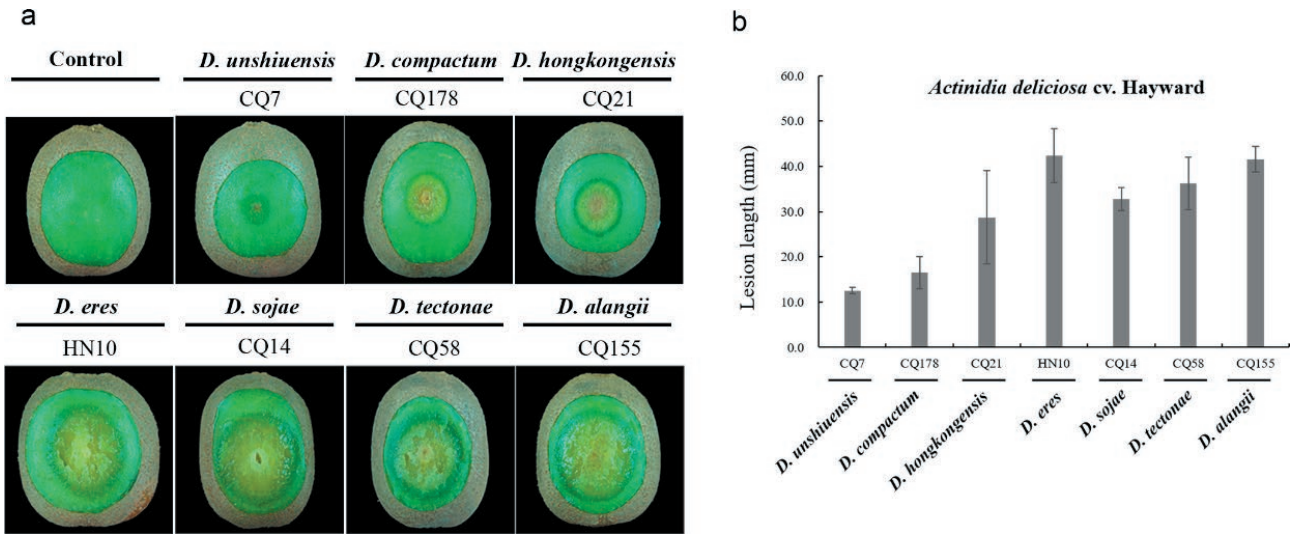

Figure 7. Symptoms and mean lesion lengths caused by inoculation of wounded kiwifruit fruits (*Actinidiae deliciosa* 'Hayward') with mycelium plugs from cultures of seven *Diaporthe* spp. a, representative symptoms photographed at 10 d post inoculation. b, mean lesion lengths (four replicates) measured at 7 d post-inoculation.

Diaporthe tectonae or *D. alangii* isolates caused large lesions (mean length = 18–39 mm), and *D. compactum*, *D. eres*, *D. hongkongensis*, *D. sojae*, or *D. unshiuensis* caused shorter lesions (5–15 mm) on *Pyrus pyrifolia* 'Cuiguan'(Figure 8a). Lesion lengths on *Prunus salicina* 'Dahongpao' caused by the seven *Diaporthe* species were of length 5–20 mm, except that two isolates caused larger lesions, with those from *D. sojae* isolate (CQ14) being 30 mm, and those from *D. alangii* isolate (SC74) being 53 mm (Figure 8b). The lesion lengths on *Malus pumila* 'Hong Fushi' caused by the seven *Diaporthe* species were mostly 5–15 mm in length, except for those from one isolate of *D. alangii* (SC74) which were longer (70 mm) (Figure 8c). The lesion lengths on *Prunus persica* 'Youtao' caused by *D. alangii* isolate CQ155, *D. compactum* isolate CQ178, *D. eres*, *D. hongkongensis*, *D. sojae*, or *D. unshiuensis* were 5–10 mm long, and those from the remaining isolates were larger (15–25 mm) (Figure 8d). *Diaporthe alangii* caused large lesions (60 mm) on *Prunus aremeniaca* 'Helanxiangxing', followed by *D. hongkongensis*, *D. eres*, *D. sojae*, *D. tectonae* isolate CQ58, or *D. unshiuensis* isolate CQ7 (15–30 mm), and the remaining isolates caused short lesions (5–10 mm) (Figure 8e). No lesions were induced in the branches inoculated with non-colonized PDA plugs.

DISCUSSION

Diaporthe spp. previously reported on kiwifruit have been associated with fruit stem-end rots (Sommer and Beraha, 1975; Hawthorne *et al*., 1982; Lee *et al*., 2001; Koh *et al*., 2005; Luongo *et al*., 2011; Thomidis *et al*., 2019), and with shoot blight and leaf spots. In the present study, a large-scale investigation of *Diaporthe* species associated with kiwifruit infections was conducted in nine major cultivation provinces of China. Multilocus phylogenetic analyses and morphological characterization of isolated fungi were employed to evaluate the diversity of *Diaporthe* species associated with shoot blight and leaf spot of kiwifruit, and pathogenicity tests was performed to fulfill Koch's postulates for representative *Diaporthe* isolates. This study has shown that seven *Diaporthe* species, including *D. unshiuensis*, *D. eres*, *D. sojae*, *D. hongkongensis*, *D. compactum*, *D. alangii*, and *D. tectonae*, were the causal organisms of shoot blight and leaf spot diseases of kiwifruit. As well, *D. unshiuensis*, *D. sojae*, *D. compactum*, *D. alangii*, and *D. tectonae* are here first reported as causes of kiwifruit shoot blight and leaf spot. The study was comprehensive, investigating samples from 16 orchards located in nine major kiwifruit production areas in China, and used phylogenetic analyses and morphology to characterize a large number of fungus isolates.

DNA sequence data are essential for resolving taxonomic questions, redefining species boundaries, and accurate species nomenclature (Guarnaccia and Crous, 2017; Guarnaccia *et al*., 2017). Phylogenetic analyses individually based on ITS, *EF1-α*, and *TUB* sequence data differentiated *D. compactum*, *D. eres*, *D. hongkongensis*, *D. sojae*, and *D. unshiuensis*. However, ITS and *EF1-α* gathered *D. tectonae* and *D. alangii* into one

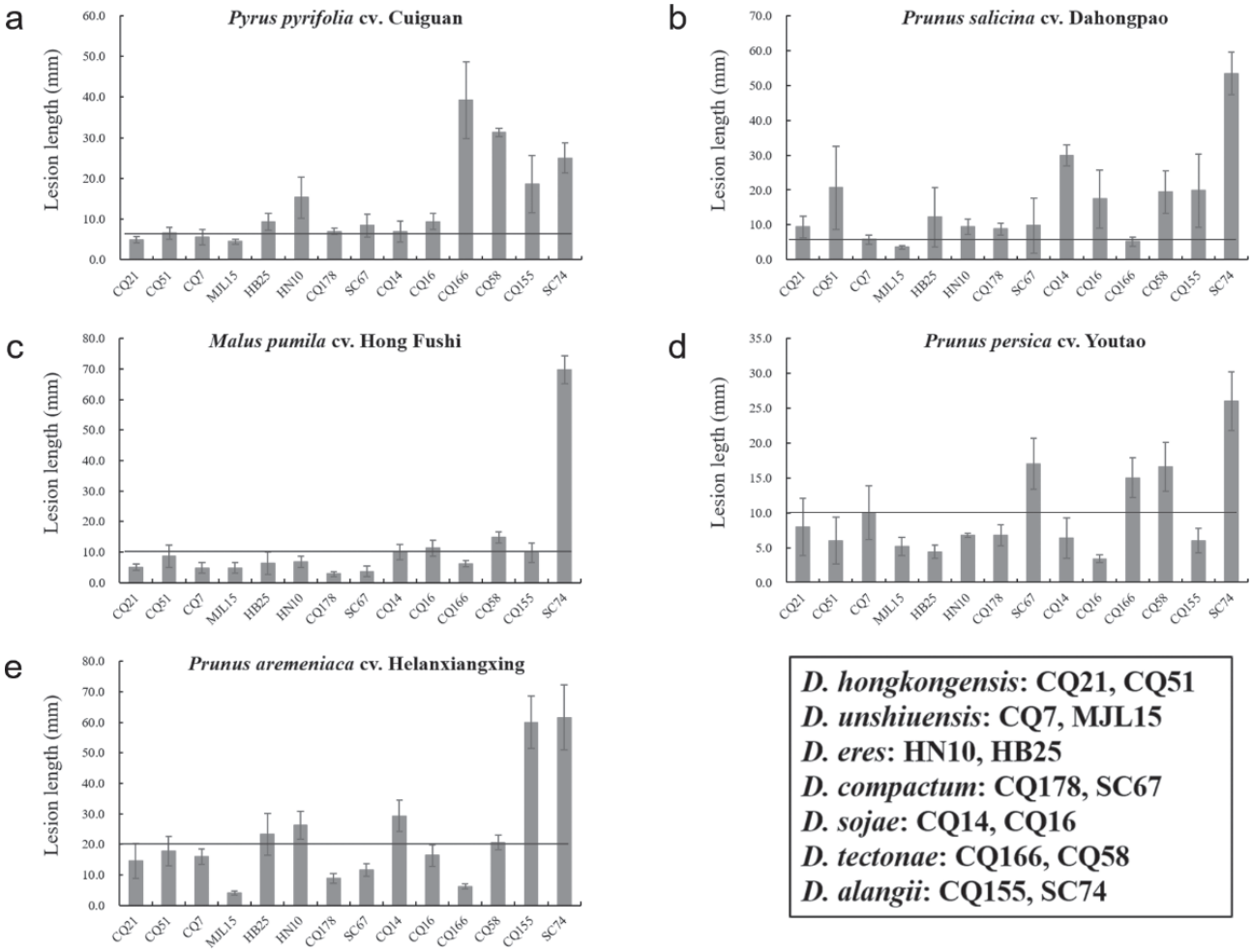

Figure 8. Mean lesion lengths on wounded shoots of pear, plum, apple, peach, and apricot, at 10 d post-inoculation, induced by mycelium plugs from cultures of representative isolates of seven *Diaporthe* species. a. lesion lengths on shoots of *Pyrus pyrifolia* 'Cuiguan', b, *Prunus salicina* 'Dahongpao', c, *Malus pumila* 'Hong Fushi', d, *Prunus persica* 'Youtao', or e, *Prunus aremeniaca* 'Helanxiangxing'.

clade. Several studies have used three to five concatenated genes simultaneously to separate species within *Diaporthe* (Santos *et al*., 2011; Gomes *et al*., 2013; Gao *et al*., 2015; Diaz *et al*., 2017). As ITS and the *EF1-α* gene have limitations for distinguishing *D. alangii* and *D. tectonae*, the concatenated ITS, *EF1-α*, and *TUB* phylogenetic analysis was successively employed to discriminate these two fungi. The results showed that the two species clustered into two clades with high bootstrap (1.00/99). These two fungi also differed morphologically, with *D. tectonae* having shorter alpha conidia than *D. alangii*.

Prevalence analyses of the seven *Diaporthe* spp. showed that the most dominant species responsible for leaf spot and branch blight of kiwifruit were: *D. unshiuensis* (100 isolates, 35.2%, isolated from Anhui, Chongqing, Fujian, Henan, Hubei, Sichuan, and Zhejiang); *D. eres* (94 isolates, 33.1%, isolated from Anhui, Chongqing, Fujian, Henan, Hubei, Shandong, Shanxi, Sichuan, and Zhejiang); and *D. sojae* (57 isolates, 20.1%, isolated from Chongqing, Fujian, Henan, Hubei, Shandong, Sichuan, and Zhejiang). The other identified fungi were less common, including: *D. honkongensis* (19 isolates, 6.7%, isolated from Anhui, Chongqing, Fujian, and Hubei), *D. compactum* (six isolates, 2.1%, isolated from Chongqing, Fujian, Hubei, and Sichuan); *D. alangii* (five isolates, 1.8%, isolated from Chongqing, Fujian, Hubei, and Sichuan), and *D. tectonae* (three isolates, 1.1%, isolated from Chongqing and Sichuan) (Table 2). Analysis of *Diaporthe* species in the sampled areas showed obvious species diversity in Anhui, Chongqing, Fujian, Hubei, Sichuan, and Zhejiang. This may be attributed to the humid and warm climate in these provinces, which is suitable for survival of *Diaporthe* spp. In contrast, only one *Diaporthe* sp. was identified from Shanxi, two from

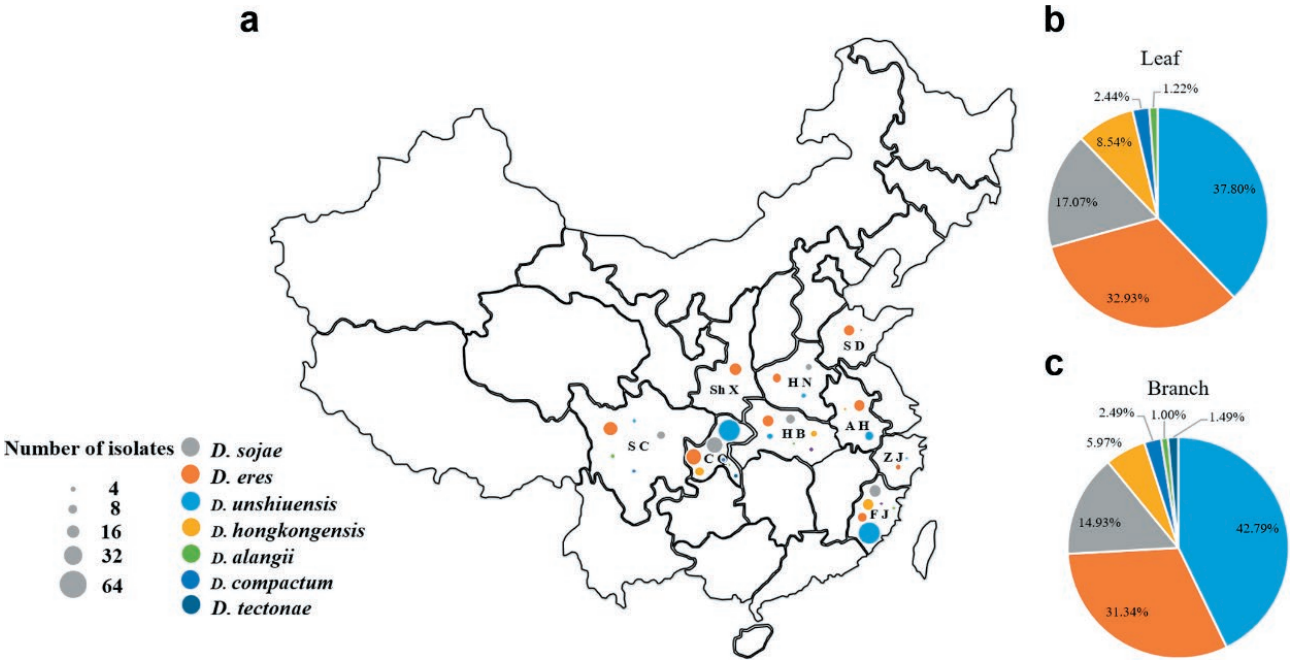

Figure 9. Sample collections of kiwifruit shoot blight and leaf spot diseases, and distribution of *Diaporthe* species in China. a, numbers and species of different *Diaporthe* species from kiwifruit plants. Each coloured circle represents one fungus species, and the size of the circle indicates the number of isolates. Abbreviations indicate provinces or regions of Anhui (AH), Chongqing (CQ), Henan (HN), Hubei (HB), Fujian (FJ), Shandong (SD), Shanxi (ShX), Sichuan (SC) and Zhejiang (ZJ). b, and c, isolation rates (%) of different *Diaporthe* spp. from kiwifruit leaf or branch tissues.

Shandong, and three species were identified from Henan (Figure 9a), which may be related to the dry climate of these three provinces being unsuitable for *Diaporthe*.

Since *Diaporthe* spp. have endophytic, saprobic or pathogenic lifestyles, pathogenicity to kiwifruit was assessed by inoculating leaves, shoots, and fruit of different kiwifruit species, using wound and non-wound inoculation methods. Wound inoculations showed that all the species were pathogenic and caused leaf spot and shoot blight of this host. The different fungi also showed significantly different virulence, with *D. alangii* and *D. tectone* as the most aggressive species, followed by *D. compactum*, *D. eres*, *D. hongkongensis*, *D. unshiuensis*, and *D. sojae*. It is significant, however, that the inoculations of these seven species on unwounded leaves, branches, and fruits did not cause disease symptoms. These species can be endophytes and opportunist pathogens occurring in a wide range of hosts and later as saprobes on dead host tissues.

Host affiliation has been for species delimitation in *Diaporthe*, but this has proved uninformative because many *Diaporthe* spp. have been recorded on a wide range of hosts (Santos and Phillips, 2009; Udayanga *et al*., 2012; Gao *et al*., 2015; Guarnaccia *et al*., 2020). For example, *D. lithocarpus* was confirmed as the cause of diseases on five plant hosts belonging to different families, and *Lithocarpus glabra* was shown to host seven different species of *Diaporthe* (Gao *et al*., 2014). In the present study, the seven *Diaporthe* species isolated from kiwifruit were not host-specific. *Diaporthe tectonae* was first reported to cause branch and twig dieback on *Tectonae grandis* in Northern Thailand (Doilom *et al*., 2016), and the present study has showed that *D. tectonae* could induce shoot blight of kiwifruit in China. *Diaporthe alangii* was originally isolated from dieback branches of *Alangium* in China (Yang *et al*., 2018b). The present study confirmed *D. tectonae* as the cause of leaf spot and shoot blight of kiwifruit. *Diaporthe eres*, *D. sojae*, and *D. hongkongensis* are pathogens causing shoot canker of grapevine and pear (Dissanayake *et al*., 2014; Guo *et al*., 2020b), as well as kiwifruit shoot blight and leaf spot (present study). *Diaporthe unshiuensis* was reported from the fruit of *Citrus unshiu* with unidentified symptoms and non-symptomatic branches and twigs of *Fortunella margarita* (Huang *et al*., 2015), and the present study showed weak aggressiveness of this species to kiwifruit. Several *Diaporthe* spp. have been recently recognized as causal agents of diseases of *Rosaceae* fruit crop plants, including peach, pear, and apple (Bai *et al*., 2015; Sessa *et al*., 2017; Tian *et al*., 2018; Guo *et*

al., 2020b). However, kiwifruit is often in mixed plantings with apple, apricot, pear, peach, and plum in many kiwifruit production areas in China. Results of host range and virulence assessments described here have shown the seven *Diaporthe* species were pathogenic, not only to kiwifruit, but also to most other *Rosaceae* fruit crop hosts. This indicates that these pathogens have the potential to infect these alternative hosts, potentially providing pathogen inoculum across these hosts.

In conclusion, identification of these pathogens provides valuable new information to assist understanding of leaf spot and branch blight of kiwifruit. The study has also shown the *Diaporthe* species responsible for these diseases, which will assist the design of potential disease prevention and management strategies for these economically important diseases.

ACKNOWLEDGEMENTS

This study was financially supported by the Key National Project (no. 2018YFD0201406) and the earmarked fund for Pear Modern Agro-Industry Technology Research System (CARS-28-16) of the Chinese Ministry of Agriculture.

LITERATURE CITED

Akilli, S., Serce, C. U., Katircioglu, Y. Z., Karakaya, A., Maden, S., 2011. Involvement of *Phytophthora citrophthora* in kiwifruit decline in Turkey. *Journal of Phytopathology* 159: 579–581.

Bai, Q., Zhai, L. F., Chen, X., Hong, N., Xu, W. X., Wang, G. P., 2015. Biological and molecular characterization of five *Phomopsis* species associated with pear shoot canker in China. *Plant Disease* 99: 1704–1712.

Bai, Q., Wang, G. P., Hong, N., 2017. First report of *Diaporthe tulliensis* and *Diaporthe actinidiae* causing kiwifruit stem canker in Hubei and Anhui provinces, China. *Plant Disease* 101: 508.

Beraha, L., O'Brien, M. J., 1979. *Diaporthe melonis* sp. nov., a new soft rot of market cantaloupes. *Journal of Phytopathology* 94: 199–207.

Carbone, L., Kohn, L. M., 1999. A method for designing primer sets for speciation studies in filamentous ascomycetes. *Mycologia* 91: 553–556.

Conn, K. E., Gubler, W. D., 1993. Bacterial blight of kiwifruit in Califorina. *Plant Disease* 77: 228–230.

Díaz, G. A., Latorre, B. A., Lolas, M., Ferrada, E., Naranjo, P., Zoffoli, J. P., 2017. Identification and characterization of *Diaporthe ambigua*, *D. australafricana*, *D. novem*, and *D. rudis* causing a postharvest fruit rot in kiwifruit. *Plant Disease* 101: 1402–1410.

Díaz, G. A., & Latorre, B. A., 2018. First report of cordon dieback of kiwifruits caused by *Diaporthe ambigua* and *D. australafricana* in Chile. *Plant Disease* 102: 446.

Dissanayake, A. J., Liu, M., Zhang, W., Chen, Z., Udayanga, D., … Kevin, D. H., 2014. Morphological and molecular characterisation of *Diaporthe* species associated with grapevine trunk disease in China. *Fungal Biology* 119: 283–294.

Doilom, M., Dissanayake, A. J., Wanasinghe, D. N., Boonmee, S., Liu, J. K., … Kevin D. H., 2016. Microfungi on *Tectona grandis* (teak) in northern Thailand. *Fungal Diversity* 82: 107–182.

Elfar, K., Torres, R., Diaz, G. A., Latorre, B. A., 2013. Characterization of *Diaporthe australafricana* and *Diaporthe* spp. associated with stem canker of blueberry in Chile. *Plant Disease* 97: 1042–1050.

Erper, I., Turkkan, M., Ozcan, M., Luongo, L., Belisario, A., 2017. Characterization of *Diaporthe honkongensis* species causing stem-end rot on kiwifruit in Turkey. *Journal of Plant Pathology* 99: 779–782.

Fan, X. L., Bezerra, J. D. P., Tian, C. M., Crous, P. W., 2018. Families and genera of diaporthalean fungi associated with canker and dieback of tree hosts. *Persoonia* 40: 119–134.

FAO, 2018. Food and Agriculture Organization of the United Nations. http://www.fao.org/faostat/en/#data/QC. Accessed 20 February 2020.

Freeman, S., Talma, T., Shabi, E., 1996. Characterization of *Colletotrichum gloeosporioides* isolates from avocado and almond fruits with molecular and pathogenicity tests. *Applied and Environmental Microbiology* 62: 1014–1020.

Fu, M., Crous, P. W., Bai, Q., Zhang, P. F., Xiang, J., … Wang, G. P., 2018. *Colletotrichum* species associated with anthracnose of *Pyrus* spp. in China. *Persoonia* 42: 1–35.

Gao, Y. H., Sun, W., Su, Y. Y., Cai, L., 2014. Three new species of *Phomopsis* in Gutianshan Nature Reserve in China. *Mycological Progress* 13: 111–121.

Gao, Y. H., Su, Y., Sun, W., Cai, L., 2015. *Diaporthe* species occurring on *Lithocarpus glabra* in China, with descriptions of five new species. *Fungal Biology* 119: 295–309.

Gao, Y. H., Liu, F., Duan, W. J., Crous, P. W., Cai, L., 2017. *Diaporthe* is paraphyletic. *IMA Fungus* 8: 153–187.

Glass, N. L., Donaldson, G. C., 1995. Development of primer sets designed for use with the PCR to amplify conserved genes from filamentous ascomycetes.

Applied and Environmental Microbiology 61: 1323–1330.

Gomes, R. R., Glienke, C., Videira, S. I. R., Lombard, L., Groenewald, J. Z., Crous, P. W., 2013. *Diaporthe*: a genus of endophytic, saprobic and plant pathogenic fungi. *Persoonia* 31: 1–41.

Guarnaccia, V., Crous, P. W., 2017. Emerging citrus diseases in Europe caused by species of *Diaporthe*. *IMA Fungus* 8: 317–334.

Guarnaccia, V., Groenewald, J. Z., Woodhall, J., Armengol, J., Cinelli, T., … Crous, P. W. 2017. *Diaporthe* diversity and pathogenicity revealed from a broad survey of grapevine diseases in Europe. *Persoonia* 40: 135–153.

Guarnaccia, V., Crous, P. W., 2018. Species of *Diaporthe* on camellia and citrus in the Azores Islands. *Phytopathologia Mediterranea* 57: 307–319.

Guarnaccia, V., Martino, I., Tabone, G., Brondino, L., Gullino, M. L. 2020. Fungal pathogens associated with stem blight and dieback of blueberry in northern Italy. *Phytopathologia Mediterranea* 59: 229–245.

Guo, Y. H., Liu, Q., He, P., 2020a. Current situtation, problems and countermeasures of kiwifruit industry in China. *Guizhou Agriculture Science* 48: 69–73.

Guo, Y. S., Crous, P. W., Bai, Q., Fu, M., Yang, M. M., … Wang, G. P., 2020b. High diversity of *Diaporthe* species associated with pear shoot canker in China. *Persoonia* 45: 135-162.

Hawthorne, B. T., Reesgeorge, J., Samuels, G. J., 1982. Fungi associated with leaf spots and post-harvest fruit rots of kiwifruit (*Actinidia chinensis*) in New Zealand. *New Zealand Journal of Botany* 20: 143–150.

Hawthorne, B. T., Otto, C., 2012. Pathogenicity of fungi associated with leaf spots of kiwifruit. *New Zealand Journal of Agricultural Research* 29: 533–538.

Hibbett, D. S., Taylor, J. W., 2013. Fungal systematics: is a new age of enlightenment at hand? *Nature Reviews Microbiology* 11: 129–133.

Hoang, D. T., Chernomor, O., Haeseler, A. V., Minh, B. Q., Vinh, L. S., 2017. UFBoot2: Improving the Ultrafast Bootstrap Approximation. *Molecular Biology and Evolution* 35: 518–522.

Huang, F., Hou, X., Dewdney, M. M., Fu, Y. S., Chen, G. Q., … Li, H., 2013. *Diaporthe* species occurring on citrus in China. *Fungal Diversity* 61: 237–250.

Huang, F., Udayanga, D., Wang, X., Hou, X., Mei, X., … Li, H., 2015. Endophytic *Diaporthe* associated with citrus: a phylogenetic reassessment with seven new species from China. *Fungal Biology* 119: 331–347.

Huang, H. W., 2009. History of 100 years of domestication and improvement of kiwifruit and gene discovery from genetic introgressed populations in the wild. *Chinese Bulletin of Botany* 44: 127–142.

Huang, S., Ding, J., Deng, D., Tang, W., Sun, H., … Liu, Y. S., 2013. Draft genome of the kiwifruit *Actinidia chinensis*. *Nat Commun* 4: 1–9.

Jeong, I. H., lim, M. T., Kim, G. H., Han, T. W., Kim, H. C., Kim, M. J., … Koh, Y. J., 2008. Incidences of leaf spots and blights on kiwifruit in Korea. *The Plant Pathology Journal* 24: 125–130.

Katoh, K., Standley, D. M., 2013. MAFFT multiple sequence alignment software version 7: improvements in performance and usability. *Molecular Biology and Evolution* 30: 772–780.

Koh, Y. J., Lee, D. H., Shin, J. S., Hur, J. S., 2001. Chemical and cultural control of bacterial blossom blight of kiwifruit caused by *Pseudomonas syringaein* Korea. *New Zealand Journal of Crop and Horticultural Science* 29: 29–34.

Koh, Y. J., Hur, J. S., Jung, J. S., 2005. Postharvest fruit rots of kiwifruit (*Actinidia deliciosa*) in Korea. *New Zealand Journal of Crop and Horticultural Science* 33: 303–310.

Kumar, S., Stecher, G., Tamura, K., 2016. MEGA7: Molecular evolutionary genetics analysis version 7.0 for bigger datasets. *Molecular Biology and Evolution* 33: 1870–1874.

Lee, J. G., Lee, D. H., Park, S. Y., Hur, J. S., Koh, Y. J., 2001. First report of *Diaporthe actinidiae*, the causal organism of stem-end rot of kiwifruit in Korea. *Plant Pathology Journal* 17: 110–113.

Li, C., Jiang, J. X., Leng, J. H., Li, B. M., Yu, Q., Tu, G. Q., 2013. Identification of pathogen causing shoot blight of kiwifruit. *Plant Protection* 24: 130–133.

Li, H., Yu, S., Tang, W., Miao, M., Liu, Y., 2019. First report of *Diaporthe passiflorae* and *Diaporthe nobilis* causing a postharvest kiwifruit rot in Sichuan province, China. *Plant Disease* 103: 771–771.

Li, L., Pan, H., Chen, M., Zhang, S., Zhong, C., 2017a. Isolation and identification of pathogenic fungi causing postharvest fruit rot of kiwifruit (*Actinidia chinensis*) in China. *Journal of Phytopathology* 165: 782–790.

Li, L., Pan, H., Liu, W., Chen, M. Y., Zhong, C. H., 2017b. First report of *Diaporthe actinidiae* causing stem-end rot of kiwifruit during post-harvest in China. *Plant Disease* 101: 1054.

Luongo, L., Santori, A., Riccioni, L., Belisario, A., 2011. *Phomopsis* sp. associated with post-harvest fruit rot f kiwifruit in Italy. *Journal of Plant Pathology* 93: 205–209.

Minh, B. Q., Schmidt, H. A., Chernomor, O., Schrempf, D., Woodhams, M. D., … Lanfear, R., 2020. IQ-TREE

2: new models and efficient methods for phylogenetic inference in the genomic era. *Molecular Biology and Evolution* 37: 1530–1534.

Mostert, L., Crous, P. W., Kang, J., Phillips, A. J. L., 2001. Species of *Phomopsis* and a *Libertella* sp. occurring on grapevines with specific reference to South Africa: morphological, cultural, molecular and pathological characterization. *Mycologia* 93: 146–167.

Mousakhah, M., Jamali, A., Khodaparast, S. A., Olia, M., 2014. Incidence of leaf spots, blights and fruit rots of kiwifruit (*Actinidia deliciosa*) in Guilan province. *Iranian Journal Plant Pathology* 50: 173–181.

Nazerian, E., Mirabolfathy, M., Ashnaei, S. P., Beiki, F., 2019. Characterization of *Botryosphaeria dothidea* as new pathogen of kiwifruit in Iran. *Journal of Plant Protection Reasearch* 59: 134–137.

Nguyen, L. T., Schmidt, H. A., Haeseler, A., Minh, B. Q., 2015. IQ-TREE: a fast and effective stochastic algorithm for estimating maximum-likelihood phylogenies. *Molecular Biology and Evolution* 32: 268–274.

Nylander, J., 2004. MrModelTest v. 2. program distributed by the author. Evolutionary Biology Centre, Uppsala University.

Pan, H., Hu, Q. L., Zhang, S. J., Zu, D., Li, L., Zhong, C. H., 2018. Kiwifruit disease investigation and pathogen identification in Liupanshui city, Guizhou province. *Plant Protection* 44: 125–131.

Pan, L., Zhao, X., Chen, M., Fu, Y., Xiang, M., Chen, J., 2020. Effect of exogenous methyl jasmonate treatment on disease resistance of postharvest kiwifruit. *Food Chem* 305: 1–8.

Pennycook, S. R., 1985. Fungal fruit rots of *Actinidia deliciosa* (kiwifruit). *New Zealand Journal of Experimental Agriculture* 13: 289–299.

Rambaut A., 2014. FigTree, v. 1.4.2. Institute of evolutionary biology. University of Edinburgh. http://tree.bio.ed.ac.uk/software/figtree/.

Rehner, S. A., Uecker, F. A., 1994. Nuclear ribosomal internal transcribed spacer phylogeny and host diversity in the coelomycete. *Phomopsis*. *Botany* 72: 1666–1674.

Ronquist, F., Huelsenbeck, J.P., 2003. MrBayes 3: bayesian phylogenetic inference under mixed models. *Bioinformatics* 19: 1572–1574.

Santos, J. M., Phillips, A. J., 2009. Resolving the complex of *Diaporthe* (*Phomopsis*) species occurring on *Foeniculum vulgare* in Portugal. *Fungal Diversity* 34: 111–125.

Santos, J. M., Vrandecic, K., Cosic, J., Duvnjak, T., Phillips, A. J., 2011. Resolving the *Diaporthe* species occurring on soybean in Croatia. *Persoonia* 27: 9–19.

Sessa, L., Abreo, E., Bettucci, L., Lupo, S., 2017. Diversity and virulence of *Diaporthe* species associated with wood. *Phytopathologia Mediterranea* 56: 431–444.

Shin, J. S., Park, J. K., Kim, G. H., Park, J. Y., Han, H. S., …Koh, Y. J., 2004. Identification and ecological characteristics of bacterial blossom blight pathogen of kiwifruit. *Research in Plant Disease* 10: 290–296.

Sommer, N. F., Beraha, L., 1975. *Diaporthe actinidiae*, a new species causing stem-end rot of Chinese gooseberry fruits. *Mycologia* 67: 650–653.

Song,Y. L., Lin, M. M., Zhong,Y. M., Chen, J. Y., Qi, X. J. ….Fang, J. B., 2020. Evaluation of resistance of kiwifruit varieties (strains) against bacterial canker disease and correlation analysis among evaluation indexes. *Journal of Fruit Science* 41: 1–15.

Thomidis, T., and Exadaktylou, E., 2010. First report of *Botryosphaeria dothidea* causing shoot blight of kiwifruit (*Actinidia deliciosa*) in Greece. *Plant Disease* 94: 1503.

Thomidiss, T., Exadaktylou, E. Chen., S. F., 2013. *Diaporthe neotheicola*, a new threat for kiwifruit in Greece. *Crop Protection* 47: 35–40.

Thomidis, T., Prodromou, I., Zambounis, A., 2019. Occurrence of *Diaporthe ambigua* Nitschke causing postharvest fruit rot on kiwifruit in Chrysoupoli Kavala, Greece. *Journal of Plant Pathology* 101: 1295–1296.

Thompson, S. M., Tan, Y. P., Young, A. J., Neate, S. M., Aitken, E. A. B., Shivas, R. G., 2011. Stem cankers on sunflower (*Helianthus annuus*) in Australia reveal a complex of pathogenic *Diaporthe* (*Phomopsis*) species. *Persoonia* 27: 80–89.

Thompson, S. M., Tan, Y. P., Shivas, R. G., Neate, S. M., Morin, L., … Aitken, E. A. B., 2015. Green and brown bridges between weeds and crops reveal novel *Diaporthe* species in Australia. *Persoonia* 35: 39–49.

Tian, Y., Zhao, Y., Sun, T., Wang, L., Liu, J., Hu, B. S., 2018. Identification and characterization of *Phomopsis amygdali* and *Botryosphaeria dothidea* associated with peach shoot blight in Yangshan, China. *Plant Disease* 102: 2511–2518.

Udayanga, D., Liu, X. Z., Crous, P. W., McKenzie, E. H. C., Chukeatirote, E., Hyde, K. D., 2012. A multi-locus phylogenetic evaluation of *Diaporthe* (*Phomopsis*). *Fungal Diversity* 56: 157–171.

Udayanga, D., Castlebury, L. A., Rossman, A. Y., Chukeatirote, E., Hyde, K. D., 2014. Insights into the genus *Diaporthe*: phylogenetic species delimitation in the *D. eres* species complex. *Fungal Diversity* 67: 203–229.

White, T. J., Bruns, T., Lee, S., Taylor, J., 1990. Amplification and direct sequencing of fungal ribosomal RNA genes for phylogenetics. *Academic Press, San Dieg* 18: 315–322.

Wu, L., Lan, J., Xiang, X., Xiang, H., Jin, Z., Liu, Y. Q., 2020. Transcriptome sequencing and endogenous phytohormone analysis reveal new insights in CPPU controlling fruit development in kiwifruit (*Actinidia chinensis*). *PLoS One* 15 (10): e0240355.

Yang, Q., Du, Z., Tian, C. M., 2018a. Phylogeny and morphology reveal two new species of *Diaporthe* from traditional Chinese medicine in northeast China. *Phytotaxa* 336: 159–170.

Yang, Q., Fan, X. L., Guarnaccia, V., Tian, C. M., 2018b. High diversity of *Diaporthe* species associated with dieback diseases in China, with twelve new species described. *MycoKeys* 39: 97–149.

Young, S. L., Hyo, S. H., Gyoung, H. K., Young, J. K., Hur, J. S., Jung, J. S., 2009. Causal agents of blossom blight of kiwifruit in Korea. *The Plant Pathology Journal* 25: 220–224.

Yue, J., Liu, J., Tang, W., Wu, Y. Q., Tang, … Zheng, Y., 2020. Kiwifruit genome database (KGD): a comprehensive resource for kiwifruit genomics. *Horticulture Research* 7: 1–8.

Zhai, L., Zhang, M., Lv, G., Chen, X., Jia, N., … Wang, G. P., 2014. Biological and molecular characterization of four *Botryosphaeria* species isolated from pear plants showing stem wart and stem canker in China. *Plant Disease* 98: 716–726.

Zhang, Z. Z., Long, Y., H, Yang, S., Li, L., Yin, X. H., 2019. Occurrence regularity and control measures of kiwifruit blossom blight of kiwifruit. *South China Fruit* 48: 159–164.

Zhou, Y., Gong, G., Cui, Y., Zhang., D., Chang, X., … Sun, X., 2015. Identification of *Botryosphaeriaceae* species causing kiwifruit rot in Sichuan province, China. *Plant Disease* 99: 699–708.

Zou, M. F., Wang, Y. X., Wang, M. F., Zhou,Y. G. Xiong, H., Jiang, J. X., 2019. First report of leaf spot on kiwifruit caused by *Didymella bellidis* in China. *Plant Disease* 104: 1–3.